Sveriges lantbruksuniversitet
Swedish University of Agricultural Sciences

Department of Soil and Environment

Geochemistry of arsenic and heavy metals in pyrite ash
– Speciation, solubility control mechanisms and geochemical modelling

Gunilla Theorin

Master's Thesis in Environmental Science
Soil and Water Management – Master's Programme

Examensarbeten, Institutionen för mark och miljö, SLU
2015:10

Uppsala 2015

SLU, Swedish University of Agricultural Sciences
Faculty of Natural Resources and Agricultural Sciences
Department of Soil and Environment

Gunilla Theorin

Geochemistry of arsenic and heavy metals in pyrite ash – Speciation, solubility control mechanisms and geochemical modelling

Main supervisor: Dan Berggren Kleja, Department of Soil and Environment, SLU
Assistant supervisors: Charlotta Tiberg, Swedish Geotechnical Institute and Department of Soil and Environment, SLU & David Bendz, Swedish Geotechnical Institute
Examiner: Jon-Petter Gustafsson, Department of Soil and Environment, SLU

EX0431, Independent Project in Environmental Science - Master´s thesis, 30 credits, Advanced level, A2E
Soil and Water Management – Master's Programme 120 credits

Series title: Examensarbeten, Institutionen för mark och miljö, SLU
2015:10

Uppsala 2015

Keywords: soil contamination, leaching tests, extractions, EDTA, kinetics, surface complexation modelling

Online publication: http://stud.epsilon.slu.se

Abstract

This thesis was part of a project at the Swedish Geotechnical Institute aiming at investigating the geochemistry of heavy metals and arsenic in pyrite ash. The specific aims with this work were to extend the knowledge on solubility control mechanisms of metals in pyrite ash and how the sorption ability of the ash was dependent on content of iron (hydr)oxides. Pyrite ash is a waste product from the roasting process of pyrite ore when producing sulphur dioxide. Sampling was performed at the former pulp mill *Bergvik sulfit* and leaching and selective extraction tests were performed on the material.

EDTA-extractable concentrations of Cd, Cu, Pb, Zn and oxalate extractable concentrations of Al, Fe and As were used as input in the geochemical equilibrium model Visual MINTEQ together with macro-cations, anions and DOC obtained from the pH leaching test. The predicted solution concentrations of Al, Fe, Cd, Cu, Pb, Zn and As from the model were compared to the pH leaching measurements.

The model predicted the concentrations of Al, Cd, Zn and Cu very well without any parameterisation. The estimates for Pb and Fe were not as well matched with the experimental data which emphasises the need for further research on filter size and colloidal particles in solution. Too few measurements above detection limit were obtained for As to get a good verification of the model.

The mechanism controlling the solution concentration at natural pH (6.5 – 7.1) for Al and Cu seemed to be precipitation of a mineral phase and for Cd, Pb, Zn and As complexation to (hydr)oxide surfaces. At alkaline pH the solution concentration of Zn was controlled by precipitation.

Overall this approach, with leaching and selective extraction tests together with geochemical modelling, seems to be promising in the risk assessment of contaminated soils.

Populärvetenskaplig sammanfattning

Med mer än 80 000 misstänkt förorenade områden i Sverige är det ett mycket utbrett och allvarligt miljöproblem. Källan till många förorenade områden kan vara gamla industrier, kemtvättanläggningar eller gruvdrift. Det är viktigt att kartlägga var föroreningarna finns och hur allvarliga de är för att avgöra om det finns behov av att åtgärda platserna.

I den här uppsatsen har markprover som tagits på ett område vid en nedlagd pappersmassaindustri undersökts. Vid tillverkningen av svaveldioxid som användes i pappersmassatillverkningen bildades en restprodukt kallad kisaska. Denna restprodukt gjorde man sig av med genom att lägga den på hög eller genom att använda den som vägutfyllnadsmaterial. Då kisaskan har högt innehåll av tungmetaller och arsenik kan det vara miljöfarligt och giftigt för människor och det är därför viktigt att undersöka hur tillgängliga ämnena är och hur stor risken är att de sprids.

Ämnena förekommer i både fast och löst form i marken men sprids främst i sin lösta form med vattnet som sitt transportmedel. Huvudsyftet med uppsatsen var att undersöka vilka processer som är styrande vid fördelningen av fast och löst form av ämnena kadmium, koppar, bly, zink och arsenik i kisaskan. De processer som är av intresse är fastläggning av de lösta ämnena till olika fasta ytor i marken (adsorption) eller att de lösta ämnena är med i formandet av nya fasta material (utfällning av mineral).

För att undersöka detta genomfördes, på Statens geotekniska institut och på Sveriges lantbruksuniversitet, en rad olika tester. Totalhalt (både fast och löst form) och mängden som lakades ur (löst form) vid olika pH-värden undersöktes. Det beräknades även hur mycket det fanns av olika ytor i marken som föroreningarna skulle kunna fastna på. Resultaten från de olika testerna användes sedan för att bygga en modell i ett datorprogram för att beräkna fördelningen av fast och löst form av föroreningarna.

Det visade sig att kisaskan innehöll totalhalter så höga att den borde klassas som en mycket allvarlig markförorening enligt de generella riktvärdena satta av Naturvårdsverket. Kisaskan innehöll även en stor andel ytor med hög förmåga att binda ämnena i marken, men den urlakade mängden översteg ändå gränsvärdet för att få läggas på en deponi för farligt avfall. Ju lägre pH-värden desto mer av ämnena förekom i sin lösta form och desto större var risken för spridning.

Modellen visade sig kunna beräkna mängden löst form ganska bra och den visade också på vilka processer som skulle kunna styra den lösta mängden. Vid höga pH värden var fastläggning en styrande process för kadmium men för zink och koppar var det bildandet av mineral. För bly och arsenik var fastläggning till fasta ytor viktigt vid både låga och höga pH-värden.

Modellen skulle kunna användas vidare för att testa olika scenarion och därmed bidra till ett bättre underlag vid riskbedömning av kisaskeförorenade områden.

Acknowledgements

I want to thank my supervisors Dan Berggren Kleja, Charlotta Tiberg and David Bendz for support and helpful comments during my work with this thesis. I also want to thank Cecilia Toomväli, technical supervisor at the laboratory of SGI, and the personnel at the laboratory for providing me with data used in this thesis. Further I want to thank Åsa Löv for helpful discussions and guidance in the laboratory, and my fellow students at SLU and my family for their encouragement throughout my thesis work.

Table of contents

1 Introduction 9

1.1 Aim and delimitations 10

1.2 Problem formulation 10

2 Theoretical framework 11

2.1 Soil contamination 11

2.2 Metal & soil properties controlling availability 12

2.2.1 Metal and arsenic speciation in soil solutions 12

2.2.2 Sorption of soils 14

2.3 Pyrite ash 15

2.4 Geochemical modelling 16

3 Materials and methods 18

3.1 Study area and soil sampling 18

3.2 Soil analyses 19

3.2.1 Total concentrations 19

3.2.2 Kinetics 19

3.2.3 Extraction of heavy metals with Na_2EDTA 20

3.2.4 Leaching tests 20

3.2.5 Extraction of iron and aluminium (hydr)oxides 21

3.3 Geochemical modelling 21

3.3.1 Speciation analysis of leachate 22

3.3.2 Controlling mineral phases 22

3.3.3 Surface complexation modelling 22

4 Results & discussion 24

4.1 Solid phase chemistry 24

4.1.1 Total concentrations 24

4.1.2 Extracted concentrations 25

4.2 Solution chemistry 33

4.2.1 Leaching test at natural pH 33

4.2.2 pH leaching test 34

4.2.3 Kinetics 39

4.3 Geochemical modelling 44

4.3.1 Solution speciation 44

4.3.2 Solubility control mechanisms 47

4.3.3 Surface complexation modelling 49

4.3.4 Comparison predicted and measured concentrations 51

5 Conclusions 61

References 63

Appendix 65

1 Introduction

The Swedish Environmental Protection Agency (SEPA) has estimated the number of contaminated sites in Sweden to around 80 000 (Naturvårdsverket, 2014). These sites are continuously being investigated and at the moment approximately 1200 of them have been assigned to hazard class 1 and are in greatest need of remediation.

In this thesis a site contaminated with pyrite ash was investigated. Pyrite ash is a waste product from the production of sulphur dioxide with the main objective for being used in the paper industry. The sulphur dioxide is produced by roasting pyrite ore (FeS_2) and the waste product, depending on the primary material, contains heavy metals and arsenic often at levels toxic to living organisms.

On the first half of the 20^{th} century it was common to discard the pyrite ash wastes on disposals near the industry or to use it as road fillings or as raw material for iron production. Large quantities of pyrite ash have been deposited on land in Sweden and the degree of contamination varies. At some sites the soil is partly contaminated with streaks of ash but in others the ash represents almost the entire "soil" matrix (Ohlsson et al., 2012).

Generic guidelines are often being used in the evaluation of contaminated sites. However, since the toxic elements in pyrite ash are embedded in the "soil" matrix it may be less available to organisms than in "ordinary" contaminated soils. More knowledge about the geochemistry of the ash is needed to better understand the behaviour of the contaminants in the environment.

Due to the large quantities disposals of pyrite ash often hold, remediation strategies can become very costly. Site specific risk assessments are important to lower the costs and to more effectively cope with the possible negative environmental impacts of the contaminant. Nevertheless, to make reliable site-specific risk assessments in order to plan for remediation strategies, in-depth knowledge about the specific mechanisms controlling the mobility and toxicity are required. In this thesis the geochemistry of pyrite ash was investigated by the use of leaching and extraction tests. The observed solubility of arsenic and the dominant heavy metals was evaluated using the equilibrium model Visual MINTEQ.

This thesis was part of a project at the Swedish Geotechnical Institute (SGI) aiming at investigating the geochemistry of pyrite ash at Bergvik.

1.1 Aim and delimitations

The aims of this thesis were to extend the knowledge on solubility control mechanisms of metals in pyrite ash and how the sorption ability of the ash was dependent on the content of iron (hydr)oxides.

The research was limited to samples taken from one pyrite ash deposit and the focus was on the major contaminants cadmium, lead, zinc, copper and arsenic.

1.2 Problem formulation

Sites contaminated with pyrite ash have increased levels of heavy metals and arsenic in the soil. Leaching of these metals to the surrounding waters might pose risks to the environment and to human health. At present there is a knowledge gap regarding the behaviour of pyrite ash which needs to be filled in order to do reliable risk assessments. Models such as Visual MINTEQ can help us interpret results from experiments to get a better understanding of how the risk might develop over time and provide a theoretical base for addressing proper remediation strategies.

2 Theoretical framework

2.1 Soil contamination

Elements present in the soil, either naturally or introduced by human activities causing pollution, may reach levels that are toxic to living organisms. For example, mining activities have enhanced the amount of many metals in soils and waters resulting in toxic levels (Sposito, 2008). One of Sweden´s 16 national environmental quality objectives is "A non-toxic environment" and included in this objective is the remediation of contaminated sites to the extent that they do not pose any threat to human health or the environment (Naturvårdsverket, 2012).

When it comes to understanding the potential toxicity of elements to plants or animals, the total content of the element in soil is usually not very useful. Another more useful parameter is the fraction related to mobility and uptake, often referred to as the element´s availability (McBride, 1994). The availability is highly affected by the solid-solution partitioning of the element where the leaching of a metal from the soil can be related to the dissolved concentration, and on the amount of metal on the solid phase buffering the concentration in solution (Degryse et al., 2009). A weak acid or a chelating complex agent can be used to estimate the potential leaching fraction (Nordbäck, et al., 2004b), which in a long term perspective could be available for uptake by living organisms.

Since the mobility of an element highly depends on its chemical form, its speciation, mechanisms in the soil and properties of the element that influence the speciation are of importance.

Such properties can be the tendency of an element to complex with organic matter, chemisorb on minerals, precipitate as insoluble sulphides, carbonates, phosphates or oxides or its tendency to co-precipitate with other minerals (McBride, 1994).

Metal cations generally have low mobility in soils since they are strongly adsorbed onto mineral surfaces and organic matter. Therefore, if a soil is rich in

clays, oxides or humus it offers many sorption sites for metal cations and lowers the mobility of the metals. Metals can also form insoluble precipitates such as oxides, carbonates and sulphides.

2.2 Metal & soil properties controlling availability

In this section metal and soil properties that are important for determining the solid-solution partitioning, and thus the availability, of the metals (and arsenic) are discussed.

2.2.1 Metal and arsenic speciation in soil solutions

An element may be present as different species in the soil solution. It can occur in soluble complexes with different ligands, either organic such as fulvic acids or inorganic such as carbonate and hydroxyl ions, depending on the content and properties of the soil solution (McBride, 1994). The element can also occur as free dissolved ions and in different oxidation states depending on the redox conditions of the solution. For arsenic, the mobility is highly dependent on its oxidation state. The more mobile and toxic form of arsenic, As^{III}, is found in arsenite and As^{V} in arsenate (Essington, 2004). The arsenite species is found in reducing environments and arsenate in oxidising environments.

The free dissolved metal ion is also a soluble complex since the metal ion is forming loose bindings to water molecules (Berggren Kleja et al., 2006). The metal ion is hydrated and this gives the charged metal ion the ability to dissolve. The more negatively charged side of the water molecule, the oxygen side, orientates towards positively charged ions such as Pb^{2+} and Fe^{3+} and creates a surrounding shell. For negatively charged ions, such as AsO_4^{3-}, the water molecule orientates the hydrogen side (more positively charged side) to the ion. The correct chemical term would thus be $Al(H_20)_6^{3+}$ for the aluminium ion. The formation of soluble complexes can be described with the general reaction:

$$aM_{(aq)}^{m+} + bL_{(aq)}^{n-} \rightarrow M_aL_{b(aq)}^{q}$$

Where M^{m+} is the free metal ion with charge m^+, L^{n-} is the free ligand ion/molecule with charge n- and $M_aL_b^q$ is the soluble complex or ion pair with the charge q (Essington, 2004). The complex becomes more stable with greater covalent character and covalent bonding may occur when the metal and the ligand are directly attached in an inner-sphere complex. For outer-sphere complexes, electrostatic attraction is holding the metal and the ligand together. The stability is also influenced by the number of bonds the metal form with the ligand. Monodentate and

bidentate ligands form one and two bonds respectively to the metal ion. Organic ligands such as the naturally occurring citric acid and the synthetic compound ethylenediaminetetraacetic acid (EDTA) may form two or more bonds to the central metal ion and are thus named multidentate or polydentate ligands. Since EDTA can form six bonds to one metal ion, the affinity for the metal ion is high and the reaction results in a stable six-ring chelate complex. This chelating effect of EDTA can be utilised in remediation practices aiming at removing heavy metals from contaminated soils (Sun et al., 2001).

In a normal soil solution the amount of different soluble complexes can be in the range of 100 to 200 and metals are part of many of them (Sposito, 2008). The most important metal complexation in waters is that with humic substances (organic acids). Humic substances can either be in dissolved form or aggregated as particles. Soluble metal complexes are formed with the dissolved form.

Soluble complexes are less bioavailable than the free hydrated metal ion which is generally the most accessible and toxic species (Berggren Kleja et al., 2006). In a risk assessment, the concentration of different species is therefore of great interest. However, soluble ligands may increase total metal concentration in solution by bringing the metals into solution as soluble complex, resulting in increasing availability to plants and microorganisms (McBride, 1994).

Many soluble ligands (for example CO_3^{2-}, OH^-, organic matter) increase in concentration with increasing pH and enhance the mobility of many metals, but at the same time metal adsorption to organic and mineral surfaces are favoured at high pH and decrease their mobility. Generally, short-term toxicity is mostly associated to the solution's free metal concentration but the long-term metal uptake is to a large degree dependent on the total dissolved concentration and the soils ability to sustain this concentration (McBride, 1994).

The metal speciation can be calculated with a chemical equilibrium model (as for example Visual MINTEQ) (Jon Petter Gustafsson, 2014). In short, low pH favour free metal cations and protonated anions, and high pH favour carbonate and hydroxyl complexes.

One way to categorize metals can be according to their binding preferences, by characterizing them as hard or soft (or borderline) depending on their electronic structure (Essington, 2004). Hard metals, or Lewis acids, are generally small sized and have low polarizability whereas it is reversed for soft metals. Polarizability is the tendency of an atom to deform its electron cloud by an electric field. Metals of hard character prefer to complex ligands, or Lewis bases, of hard character, and soft metals prefer to complex soft ligands. A complex with a metal and ligand of hard character creates a strong electrostatic bond (outer-sphere complex) while a metal and ligand of soft character creates a strong covalent bond (inner-sphere complex) and the stability of the complex involving soft species will be greater.

Borderline metals shows to some degree preferences for both hard and soft ligands. In Table 1 examples of hard, borderline and soft acids and bases are shown.

Table 1. *Metals and ligands characterised as hard, soft or borderline (Essington, 2004). Metals investigated in this thesis are marked with bold.*

	Metals/Lewis acids	Ligands/Lewis bases
Hard	Ca^{2+}, Na^{+}, K^{+}, Mg^{2+}, Mn^{2+}, Fe^{3+}, As^{3+}, Al^{3+}	H_2O, OH^-, O^{2-}. CO_3^{2-}, NO_3^-, SO_4^{2-}
Borderline	Ni^{2+}, **Cu^{2+}**, **Zn^{2+}**, **Pb^{2+}**, Fe^{2+}	NO_2^-, SO_3^{2-}, Br^-, Cl^-
Soft	**Cd^{2+}**, Hg^{2+}, Cu^{+}	S^{2-}, I^-,

The dominating species in soil solutions are hard acids and bases and they are also generally the least toxic to living organisms (Essington, 2004). The most toxic species are generally the soft followed by the borderline species. Oxidation of a metal ion often results in a decreased softness and toxicity; the reduced specie Fe^{2+} is for example a borderline metal while the oxidised Fe^{3+} is a hard metal.

2.2.2 Sorption of soils

Sorption transfers ions from the solution phase to the solid phase (McBride, 1994). In soils many sorption reactions occur which will remove ions from the water and slow down its movement. Sorption includes both adsorption (such as surface complexation and ion exchange) and precipitation. The difference between the two processes is that precipitation results in three-dimensional growth of the crystal structure, whereas adsorption is only a surface process (Essington, 2004). Adsorption processes occur at the mineral surfaces at the interface of a solid and the solution phase.

Ions may be adsorbed onto oppositely charged surface groups on oxides, clay minerals and organic matter present in the soil (Essington, 2004). The charge of the surface groups may be permanent (clays) or pH-dependent (oxides and organic matter). On a pH-dependent surface a high pH results in deprotonation and more negatively charged surface groups, which will favour surface complex with positively charged ions. Surface complexation of negatively charged ions, on the other hand, is favoured at low pH. The fraction of a metal that is adsorbed is not only dependent on quantity of surface sites but also on the metals ability to form surface complexes and on the amount of other competing ions.

The reactivity of iron and aluminium (hydr)oxides are dependent on the number of reactive sites (McBride, 1994). Due to their disordered structure, amorphous minerals are more reactive compared to long-range-ordered crystalline minerals. Lead, Cu and As are strongly bound to surfaces of Fe and Al oxides. Since humic

substances (organic matter) have the ability to bind metal cations at lower pH than iron oxides, they are most important as adsorbents of cations in most Swedish soils (Berggren Kleja et al., 2006). Increased pH favour the dissolved form of organic matter (DOC). Copper and Pb have a high affinity for binding to soil organic matter (Ashworth and Alloway, 2008).

A precipitate only forms when the concentration of the components involved in the formation is sufficiently large (Berggren Kleja et al., 2006). The concentrations, or more correctly the activities, are large enough when the ion activity product (IAP) is at least as high as the solubility product for the precipitate. A precipitate could thus, to a certain extent, regulate the concentration of the free metal ion. As mentioned previously, complex forming substances also affect the concentration of free metal ions as they may form soluble complexes with the metal, and the forming of a precipitate may thus be counteracted by large quantities of complex forming substances.

Some soils provide environments more favourable to precipitation of minerals. High pH favours oxide, hydroxide and carbonate precipitates and reducing condition favours the forming of insoluble sulphide minerals (McBride, 1994).

2.3 Pyrite ash

Earlier investigations of pyrite ash have concluded that it contains high levels of heavy metals and arsenic and if produced today, it would be considered as hazardous waste that in many cases would need to be stabilized before deposited (Nordbäck et al., 2004a). The concentrations of toxic elements in the ash showed large variations between different sampling points and waste deposits, and therefore the authors suggested that site specific risk assessments are necessary.

The same investigation found that samples collected from under water generally contained more leachable metals than samples from land. The water samples also had higher amounts of sulphide minerals and lower redox potential.

Lin and Qvarfort (1996) found in their study that 70-80 % of the residue from roasted pyrite consisted of the iron oxides hematite and maghemite and less than 10 % of the material was residual sulphides such as pyrrhotite and sphalerite. The authors concluded that these sulphide minerals were the long term source of heavy metals, sulphate and acidity to the environment and the leachates from the waste were characterised by high concentrations of Zn, Fe and SO_4. The minerals controlling the concentration of Zn in the leachate seemed to be sphalerite, Zn oxides and Zn sulphate.

Álvarez-Valero et al. (2009) also concluded that sulphide minerals containing metals pose a risk to the environment when the minerals get oxidized and enables the release of metals.

2.4 Geochemical modelling

Geochemical models are important tools for understanding geochemical conditions in soils and they may be useful when conducting risk assessments for contaminated sites. The models can estimate the proportion of free metal ions which are the species that are most bioavailable and toxic. The models are also helpful for understanding the processes controlling the dissolution of the metals in the specific soil.

Visual MINTEQ (VM), the program used in this thesis, is a chemical equilibrium model which can calculate metal speciation, including solution chemistry, sorption to surfaces and precipitation/dissolution of minerals (Jon Petter Gustafsson, 2014). VM calculates saturation indices for different minerals and this provides the user with information about which minerals that are supersaturated or under saturated with respect to the concentrations in solution. This is of interest when investigating which minerals that could control the solubility of different metals. The saturation index is calculated with the following formula:

$$\mathrm{SI} = \log IAP - \log Ks$$

where IAP is the ion activity product and K_s the solubility product (Zhu and Anderson, 2002). If the ion activity product and the solubility product are almost equally large (SI = 0), it implies that the precipitation may control the concentration of the metal (which is part of the mineral) in solution. However, the SI does not provide information about at which rate this reaction occurs.

Geochemical equilibrium models can take competition of surface sites into account (Mason, 2013). This also includes competition between anions and cations for the sites at the intermediate pH interval where both anions and cations may compete for surface sites. Sorption of ions to the surfaces is further taken into consideration in the calculations since it changes the charge and potential of the surfaces.

Multisurface models combine several models to describe the distribution of sorption to solid and dissolved organic matter, (hydr)oxides and clay minerals (Degryse et al., 2009). Sorption to (hydr)oxide surfaces is calculated with a surface complexation model whereas an ion exchange method is used for sorption to clay minerals. Examples of models calculating sorption to organic matter are the Nica-Donnan and Stockholm Humic Model (SHM). In this thesis the SHM model was used. SHM has seven parameters that describe the proton dissociation reaction (Gustafsson et al., 2003). These parameters are adjustable but generic values, that are valid for average HA and FA contents, can be used.

The surface complexation model used in this thesis was a CD-MUSIC model developed by Tiberg et al. (2013).

Geochemical equilibrium models assume that the systems investigated are in equilibrium. A system is at equilibrium if none of its properties change with time (Zhu and Anderson, 2002). However, natural systems are constantly under changing conditions and therefore a truly equilibrium state is not reached. Geochemical models may still be useful for defined areas and part of systems where equilibrium can be acceptable assumed.

Another limitation with the models is that they do not provide information about how fast the processes will occur. Since processes may be rate-limited, a mineral predicted to precipitate or dissolve under certain conditions may not happen in the real world (Zhu and Anderson, 2002).

The use of selective chemical extractions (for determining amount of reactive surfaces) and pH dependent leaching tests together with multisurface modelling (without adjusting the generic parameters), have earlier proven to be successful in predicting the metal leaching from contaminated soils (Dijkstra et al., 2004, 2009).

3 Materials and methods

3.1 Study area and soil sampling

Sampling was performed by employees at the Swedish Geotechnical Institute (SGI) in the area of the former pulp mill *Bergvik sulfit* located in Söderhamn municipality year 2013 (Figure 1). The pulp mill was in operation between the years 1905 and 1979 and during a period between the 40´s and the middle of the 60´s, pyrite ash wastes were deposited along Lake Smalsjön (Nordbäck, J. et al., 2004a). In some areas the thickness of the deposition measured up to several meters and the total amount of pyrite ash was estimated to be 110 000 m^3.

Samples were taken at three different depths in two soil pits, resulting in six different sampling points; *Bergvik 1:1, 1:2, 1:3* and *2:1, 2:2, 2:3*. In Table 2 and 3 coordinates and depths for the sampling points are presented.

Table 2. *Coordinates for all sampling points.*

Sample pit	X	Y	Z-Surface level	Z-Sample level 1	Z-Sample level 2	Z-Sample level 3
1	6793156.4	597295.7	49.14	47.77	47.23	46.32
2	6793221.9	597325.4	48.67	48.44	47.32	46.42

Table 3. *Sample number and depth from surface (m).*

Sample	1:1	1:2	1:3	2:1	2:2	2:3
Depth (m)	1.37	1.91	2.82	0.23	1.35	2.25

Figure 1. Sampling in a pyrite ash deposit at *Bergvik sulfit* (Bendz, D., 2013)

3.2 Soil analyses

Soil tests were conducted both at the laboratory of SGI and at the Swedish University of Agricultural Sciences (SLU). Analyses were performed by accredited laboratories at ALS Scandinavia AB with ICP methods.

3.2.1 Total concentrations

The pyrite ash was sent to ALS Scandinavia AB for a total concentration analysis. To determining the concentration of As, Cd, Co, Cu, Hg, Ni, Pb, S and Zn the samples were dried at 50°C and dissolved with HNO_3/HCl/HF in a closed vessel in a microwave. Other elements (for example Al and Fe which were investigated in this thesis) were determined by lithium metaborate melting and dissolution with HNO_3 (ALS Scandinavia, 2015).

3.2.2 Kinetics

A kinetics study was conducted at the lab of SLU on sample 2:1 to study the effects of time on reaction development. The study was conducted on samples at both natural pH (ca. 6.4) and at lowered pH (ca. 4). Duplicates were used for all samples and the material used was field moist and sieved through a 2 mm sieve. To take the soil water content into consideration when adding solutions to the samples, a dry weight analysis on the sieved material was made.

For the dry weight analysis, a known mass of soil was dried overnight at 105 °C. The sample was cooled, the weight noted and after another hour in the oven the weight was noted again. The constant mass was then considered to be the total solids (TS) of the sample.

To 3 g of TS, 10mM $NaNO_3$ – and 20 mM HNO_3 – solutions (for samples with lowered pH), were added to obtain a total liquid content of 30 mL and a liquid to solid ratio (L/S) of 10 L/kg. The samples were placed in an end-over-end shaker for 5, 30, 62 or 91 days.

After the specified time in the shaker, the samples were centrifuged at 2700 g for 20 minutes and pH was measured on the supernatant. Prior to DOC and metal analysis the supernatant was filtered through 2 µm syringe filter. To conserve the metals 1% of concentrated HNO_3 was added to the samples analysed for metals. The samples were stored in a cooling room (maximum 8°C) until analysis.

3.2.3 Extraction of heavy metals with Na_2EDTA

The synthetic chelating agent Na_2EDTA was used to extract heavy metals more strongly bound in the soil matrix. The extracted fraction was regarded as the "geochemical active" fraction of Zn, Cd, Cu and Pb in Visual MINTEQ and represented thus the fraction which could participate in chemical reactions. The study was conducted at the lab of SLU on duplicate soil samples from all 6 sampling points. The soil was sieved through a 2 mm sieve and added field moist to the centrifugation tubes. The 0.05 M Na_2EDTA -solution was added to the tubes using an L/S ratio of 10 and the samples were shaken on an overhead shaker for 2 h. Samples were then centrifuged for 20 minutes at 2700 g and the supernatant was filtered through 2 µm syringe filter, diluted 10 times with 1 % HNO_3 -solution and stored at a maximum of 8°C prior to analysis.

3.2.4 Leaching tests

Leaching tests were performed at the lab of SGI in Linköping and analysed at ALS Scandinavia AB.

With natural pH

On sample 1:2 and 2:2 one-step batch tests with water as a leaching agent were made. The tests were performed according to the standards of SS-EN 12457-2 (Swedish Standards Institute, 2003) with one exception; the samples were shaken for 5 days (instead of 1 day). The L/S ratio used was 10 L/kg. After completion of the leaching tests, the samples were centrifuged and the supernatants were filtrated through a 0.45 µm cellulose acetate filter.

pH dependent batch tests

The laboratory at SGI conducted pH-dependent batch tests according to SS-EN 14429 (Swedish Standards Institute, 2015) on sample 1:1, 1:3, 2:1 and 2:3. The batch tests were conducted at LS 10 at various pH values by adding HNO_3 and NaOH. The samples were shaken for 5 days after the final adding of acid or base. After completion of the leaching tests, the samples were centrifuged and the supernatants were filtered through a 0.45 µm cellulose acetate filter.

Prior to the pH batch tests, a test with continuous adjustment of the pH was made on sample 2:1 according to the standard SS-EN 14997 (Swedish Standards Institute, 2015), to obtain information about the amount of acid and base needed to arrive at the requested pH values.

The results from the pH-dependent batch tests, which gave information about element content at 8 different pH values (~ pH 2 – 10), were used as input in VM to get information about solubility control mechanisms.

3.2.5 Extraction of iron and aluminium (hydr)oxides

To determine the amount of (hydr)oxides present in the ash, extractions aiming at extracting different forms of Fe and Al were performed. The extractions were conducted at the laboratory of SGI in Linköping, on all samples and according to the following standards:

- SS-EN ISO 12782-1 (Swedish Standards Institute, 2012a), which determines the content of reactive iron in the form of amorphous iron (hydr)oxides with ascorbic acid,
- SS-EN ISO 12782-2 (Swedish Standards Institute, 2012b), which determines the content of reactive iron in the form of crystalline iron (hydr)oxides with dithionite (dithionite extracts both amorphous and crystalline iron (hydr)oxides. Therefore when determining the crystalline content, the amorphous fraction determined with ascorbic acid is subtracted from the total extracted.),
- SS-EN ISO 12782-3 (Swedish Standards Institute, 2012c), which determines the content of reactive aluminium in the form of aluminium (hydr)oxides with ammonium oxalate.

3.3 Geochemical modelling

The free software Visual MINTEQ version 3.1 was used when modelling the results from the experiments.

3.3.1 Speciation analysis of leachate

As mentioned previously, VM can be used to calculate which species that is present in a solution. By using data from the leaching test as input in the program it calculates the distribution of species in that specific solution. Results from the leaching test were used as input data. Binding to dissolved organic matter was modelled with the Stockholm Humic Model. The default values were used for calculating the amount of active DOM and fraction of fulvic acid (FA) (Table 4). Since it can be assumed that colloidal particles of iron are in the analysed suspension (Pédrot et al., 2008) the mineral ferrihydrite was added as a possible solid which could control the activity of iron in solution. The measured dissolved inorganic carbon (DIC) concentrations were assumed to be carbonate. Different parameters and their respectively values can be seen in Table 4.

Table 4. *Parameters and their respectively value used in VM for speciation of elements*

Parameter	Value
Temperature	22 °C
pH	Measured
Active DOM	1.65 * DOC
% of active DOM that is FA	100
Activity of Fe^{3+}	Controlled by ferrihydrite, log K_s = 3.2

3.3.2 Controlling mineral phases

Measured concentrations of elements in the leachate water from the pH leaching tests were used as input data in the program to get information about saturation indices for different minerals. Elements with concentrations lower than the detection limit were set to half the value of the detection limit or not used at all if considered irrelevant for the reactions. Ferrihydrite was added as a possible solid that could control the free iron concentration.

The minerals that were close to, or in, equilibrium were considered as a possible mineral phase controlling the concentrations of the included elements and further investigated in the program.

The results from the kinetics study were also evaluated in this way.

3.3.3 Surface complexation modelling

In the next step the solids of interest (which could control the metal concentrations) were added to the program as possible solids (Table 5). This means that if the solid was oversaturated it was allowed to precipitate and was thus controlling the concentration of the element. The amount of active (hydr)oxide surfaces was determined from the oxalate extraction. All iron extracted with oxalate was as-

sumed to be ferrihydrite and the concentration was recalculated to represent the ferrihydrite concentration. The molecular weight of ferrihydrite used in the calculations was 106.9 g/mol and taken from the VM database.

For sorption to soil organic matter (SOM), the amount of fulvic and humic acids needed to be estimated. The SOM content was assumed to be twice the TOC concentration and of the SOM half was considered as being active. The active fraction was in turn assumed to consist of equal parts fulvic and humic acids.

Furthermore, measured concentrations of Cd, Cu, Pb and Zn from the EDTA-extraction and measured As and Al concentrations from the oxalate extraction were added to the program representing the geochemically active concentrations. These concentrations were thus available to take part in chemical reactions such as sorption and precipitation. Since ferrihydrite precipitated over the whole pH-range, it could be added as an infinite solid to make the work load for the program less heavy. The geochemical active concentrations of the macro cations (Ca, Mg, Ba, K) were taken from the lowest pH values from the pH-dependent leaching tests and the amount of dissolved organic carbon (DOC), CO_3^{2-} and SO_4^{2-} were set as fixed from the leachate of the batch test. The temperature was set to 22°C to represent the temperature in the laboratory where the tests were conducted. All parameters and their respectively value are presented in Table 5.

Table 5. *Parameters and their respectively value used in the surface complexation modelling in VM. *This parameter was later excluded in the modelling.*

Parameter/component	Value/model
Temperature	22 °C
pH	Fixed at pH stat values
Active DOM	1.65 * DOC
% of active DOM that is FA	100
Activity of Fe^{3+}	Controlled by ferrihydrite, log $*K_s$ = 3.2
Activity of Al^{3+}	$Al(OH)_3$ (soil) added as possible solid
Activity of Zn^{2+}	$Zn(OH)_2$ (epsilon) added as possible solid
Activity of Cu^{2+}	Tenorite (c) added as possible solid
Cd, Cu, Zn, Pb	EDTA-extractable
As, Al	Oxalate-extractable
Ca, Mg, Ba, K	Fixed at the value obtained from the lowest pH in the pH stat test
Na, NO_3	Added concentrations in pH stat test (corrected to get a charge balance difference <10 %)
DOC, SO_4^{2-}	Fixed as total dissolved from pH stat values
CO_3^{2-}	Fixed as total dissolved from DIC pH stat values
HFO	Ferrihydrite calculated from oxalate extractable Fe, CD-MUSIC (Tiberg et al., 2013)
SOM*	FA/HA: 25% of SOM (= 2×TOC), Stockholm Humic Model

4 Results & discussion

4.1 Solid phase chemistry

In this section the solid phase chemistry of the pyrite ash and the investigated elements are presented and discussed in the subsections total and extracted concentrations.

4.1.1 Total concentrations

The total content of the elements As, Cd, Cu, Pb and Zn in the analysed pyrite ash is presented in Table 6. A comparison with the levels of uncontaminated soils (Table 7) collected from around the world indicates the degree of contamination. If comparing the levels in the pyrite ash with the highest levels in the range of uncontaminated soils, the levels in the pyrite ash are at least ten times greater. However, this does not provide us with enough information to decide whether the levels pose any risk to the surrounding environment or not since the availability of the elements are not considered. The amount of Fe in the ash (41-46 %) is also around ten times the content in "normal" soils. The total organic carbon in the ash is varying between less than 0.03% (layer 2:3) and 0.56 % (layer 1:1).

The generic guideline values for contaminated soils from the Swedish Environmental Protection Agency (SEPA) are separated into sensitive land use and less sensitive land use. Their respective values for As, Cd, Cu, Pb and Zn can also be seen in Table 6. All elements investigated in this thesis exceed the guideline values for sensitive and less sensitive land use. Moreover, all elements but Cd exceed the generic values for less sensitive land use more than 10 times and should therefore be regarded as a very severe soil contaminant (Naturvårdsverket, 1999).

Table 6. *Average, min and max, and standard deviation of the total content of As, Cd, Cu, Pb and Zn in mg/kg and Fe and TOC in percentage. Values based on all six samples (pH based on four samples). Generic guideline values for contaminated soils in mg/kg given for sensitive land use and less sensitive land use ("Riktvärden för förorenad mark," n.d.)*

	Pyrite ash				General guideline values	
Element	Average	Min	Max	Std dev	Sensitive	Less sensitive
As	657	281	2 230	706	10	25
Cd	103	40	152	36	0.5	15
Cu	3 890	3 040	4 800	694	80	200
Pb	8 470	6 360	10 600	1 510	50	400
Zn	29 100	13 200	37 900	8 020	250	500
Fe (%)	44	41	46	1.5		
TOC (%)		<0.03	0.56			
pH	6.8	6.5	7.1			

Table 7. *Elemental content of uncontaminated soils worldwide in mg/kg (Essington, 2004)*

Element	Median	Range
As	6.00	0.1 - 40
Cd	0.35	0.01 - 2
Cu	30	2 - 250
Pb	35	2 - 300
Zn	90	1 - 900
Fe (%)	4	2 – 5.5

4.1.2 Extracted concentrations

Below the results from the different extractions are presented and discussed.

Iron

In Figure 2a and b the total amount and extracted amounts of Fe with different methods can be seen for *Bergvik 1* and *2*.

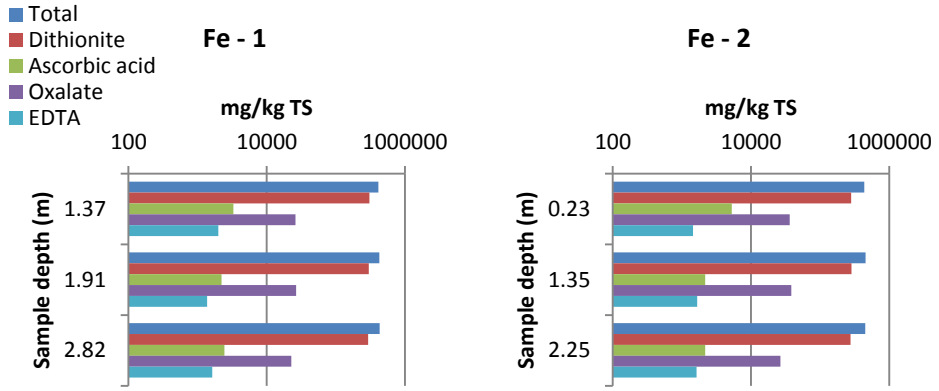

a b

Figure 2. Total amount and amount extracted Fe with dithionite, ascorbic acid, ammonium oxalate and Na_2EDTA for a) *Bergvik 1* and b) *Bergvik 2* at different depths from the surface (m). Total amount based on one sample. Extracted amounts are average values from duplicate samples.

The total and extracted amounts and seem to be quite similar both for the two sampling pits and between the three different depths. The amount Fe extracted differs however between the different methods. The largest fraction (61-74%, Table 8) is extracted with dithionite, which is used for determining the fraction of crystalline iron (hydr)oxides. Analyses with EXAFS (Tiberg, unpublished material) and XRD (Bendz, unpublished material) also show that crystalline iron (hydr)oxides predominate in the form of the mineral hematite. This is also in line with the results previously mentioned from Lin and Qvarfort (1996), that 70 – 80 % of the ash studied in their experiment constituted of iron oxides.

Table 8. *Total concentration in mg/kg TS and extracted concentrations of Fe with dithionite, ascorbic acid, ammonium oxalate and Na_2EDTA in mg/kg TS and as percentage of the total concentration.*

Sampling point	Depth (m)	mg/kg TS					% of total			
		Tot	Dit	Asc	Ox	EDTA	Dit	Asc	Ox	EDTA
1.1	1.37	413000	306000	3300	26200	2010	74	0.8	6.3	0.5
1.2	1.91	425000	299000	2230	26500	1380	70	0.5	6.2	0.3
1.3	2.82	429000	292000	2450	22800	1620	68	0.6	5.3	0.4
2.1	0.23	437000	280000	5290	36200	1440	64	1.2	8.3	0.3
2.2	1.35	456000	283000	2170	38400	1660	62	0.5	8.4	0.4
2.3	2.25	449000	274000	2170	26600	1640	61	0.5	5.9	0.4
Average		435000	289000	2930	29400	1620	67	0.7	6.8	0.4

The second largest fraction (5-8 %) is extracted with ammonium oxalate. This method is according to the standards used for extracting Al (hydr)oxides. Oxalate can however also be used to estimate the amount of ferrihydrite in the soil (Parfitt

and Childs, 1988). Since this mineral is an amorphous Fe (hydr)oxide with large specific surface area, it can play a significant role in determining the soils characteristics. According to the standards, ascorbic acid should be the extracting agent used when determining the content of amorphous Fe (hydr)oxides. This agent extracted less than 1 % of the total Fe content in the pyrite ash, or approximately 10 % of the oxalate-extractable fraction. This means that dependent on which extraction method being used, the estimated content of ferrihydrite may vary one order of magnitude. In Table 9 the calculated concentration of ferrihydrite for both the oxalate and the ascorbic acid-extractable fractions can be seen.

Table 9. *Calculated concentration of ferrihydrite in g/l from oxalate and ascorbic acid extractable iron concentration.*

Sampling point	Oxalate	Ascorbic acid
1.1	5.01	0.63
1.2	5.07	0.43
1.3	4.36	0.47
2.1	6.93	1.01
2.2	7.35	0.41
2.3	5.09	0.41

Aluminium

Total and oxalate-extractable concentrations of Al are presented in Table 10. The oxalate extractable fraction are according to the standards representing the content of reactive Al in the form of Al (hydr)oxides. The Al concentration extracted is on average 475 mg/kg TS or 0.017 moL/kg TS. This can be compared to the oxalate extractable Fe which is on average 29400 mg/kg TS or 0.53 moL/kg TS. The content of Al (hydr)oxides are thus much lower than the amorphous Fe (hydr)oxides and therefore seems to be less important as a sorbent in the ash.

Table 10. *Total concentration in mg/kg TS and extracted concentration of Al with ammonium oxalate in mg/kg TS and as percentage of the total concentration.*

Sampling	Depth	mg/kg TS		% of total
point	(m)	Total	Oxalate	Oxalate
1.1	1.37	6090	426	7.0
1.2	1.91	6250	544	8.7
1.3	2.82	3460	423	12.2
2.1	0.23	4630	528	11.4
2.2	1.35	4030	396	9.8
2.3	2.25	5100	515	10.1
Average		4927	472	10

Cadmium

Figure 3 presents the total concentration of Cd and the extracted concentration with 0.05 M Na_2EDTA. The extracted fraction differs between the different sampling points and is in the range 8.5 – 38 % of the total (Table 11). This fraction is regarded as the geochemically active fraction and thus the fraction taking part in chemical reactions. On average a third of the total Cd is regarded as active. A review article have found that the isotopically exchangeable fraction, which is the fraction of metals that are in dynamic equilibrium with metals in solution, determined with isotope dilution generally range between 40 and 80 % for Cd in field soils (Degryse et al., 2009). The extracted fraction from the pyrite ash is thus lower than the range earlier studied from normal soils, even though it has been shown that EDTA extracts more than the method determining the isotopically exchangeable fraction (Nakhone and Young, 1993).

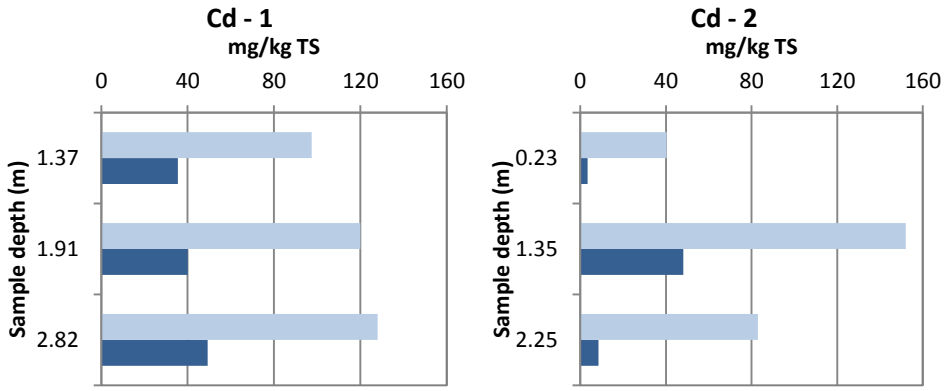

a b

Figure 3. Total Cd concentration and concentration extracted with 0.05 M Na_2EDTA for a) *Bergvik 1* and b) *Bergvik 2* at different depths from the surface (m). Total amount based on one sample. Extracted amounts are average values from duplicate samples.

Table 11. *Total and extracted concentration of Cd with 0.05 M Na_2EDTA in mg/kg TS. Extracted concentration also as percentage of the total concentration.*

Sampling point	Depth (m)	TOT mg/kg TS	EDTA mg/kg TS	EDTA % of total
1.1	1.37	98	35	36
1.2	1.91	120	40	33
1.3	2.82	128	49	38
2.1	0.23	40	3.4	8.5
2.2	1.35	152	48	32
2.3	2.25	83	8.5	10
Average		103	31	26

There is no clear relationship with total content or amount extracted with sample depth. For sample pit 1 it seems like the total (and extracted) concentration is increasing with increasing depth, however this pattern cannot be seen for sample pit 2 where the highest concentration is found in the middle layer.

Copper

In Figure 4 the total and extractable concentrations of Cu with Na_2EDTA can be seen. EDTA extracts between 45 and 63 % of the total (Table 12) and on average about half is being extracted. The result imply that on average about half of the total Cu is being active and may participate, in a long term perspective, in chemical reactions. The isotopically exchangeable fraction for uncontaminated and contaminated soils generally range between 4 and 52 % (average 20 %) (Degryse et al., 2009).

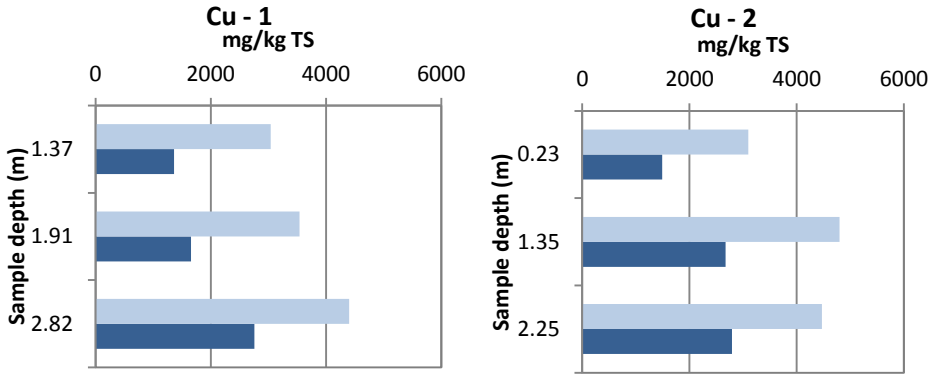

a b

Figure 4. Total Cu concentration and concentration extracted with 0.05 M Na_2EDTA for a) *Bergvik 1* and b) *Bergvik 2* at different depths from the surface (m). Total amount based on one sample. Extracted amounts are average values from duplicate samples.

Similar to Cd, the total concentration of Cu is increasing with increasing depth in sample pit 1 but the highest concentration in sample pit 2 is found in the middle layer.

Table 12. *Total and extracted concentration of Cu with 0.05 M Na_2EDTA in mg/kg TS. Extracted concentration also as percentage of the total concentration.*

Sampling point	Depth (m)	TOT mg/kg TS	EDTA mg/kg TS	EDTA % of total
1.1	1.37	3040	1360	45
1.2	1.91	3540	1650	47
1.3	2.82	4400	2760	63
2.1	0.23	3100	1490	48
2.2	1.35	4800	2670	56
2.3	2.25	4470	2790	62
Average		3900	2100	53

Lead

The total and the EDTA-extractable concentrations for Pb are presented in Figure 5 and Table 13. For layer 1:1 EDTA extracts 99 % of the total content and for the rest between 64 – 86 %. For lead the active fraction is thus close to the total content for some layers. On average three quarters of the total concentration is available for participating in reactions. The isotopically exchangeable fraction of Pb in contaminated soils have been found to be larger than 40 % (Degryse et al., 2009).

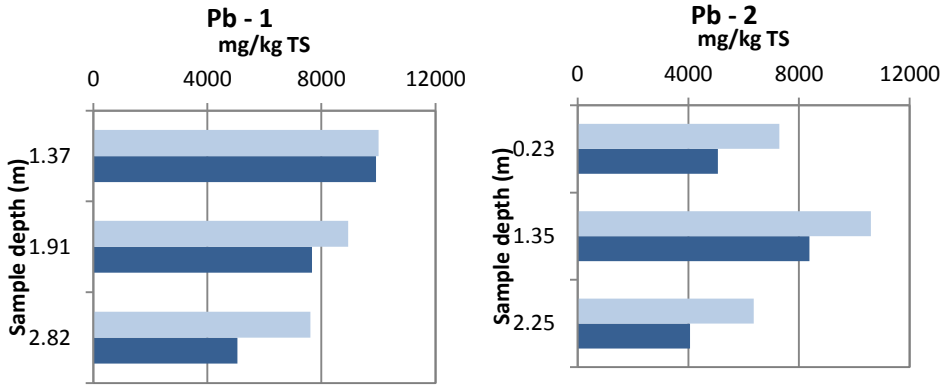

a *b*

Figure 5. Total Pb concentration and concentration extracted with 0.05 M Na_2EDTA for a) *Bergvik 1* and b) *Bergvik 2* at different depths from the surface (m). Total amount based on one sample. Extracted amounts are average values from duplicate samples.

The total lead content is decreasing with increasing depth for sample pit 1, which is opposite to the trend for Cd and Cu in this pit. Similar to Cd and Cu the highest content is found in the middle layer in sample pit 2.

Table 13. *Total and extracted concentration of Pb with 0.05 M Na_2EDTA in mg/kg TS. Extracted concentration also as percentage of the total concentration.*

Sampling point	Depth (m)	TOT mg/kg TS	EDTA mg/kg TS	EDTA % of total
1.1	1.37	10000	9920	99
1.2	1.91	8940	7670	86
1.3	2.82	7610	5060	66
2.1	0.23	7290	5060	69
2.2	1.35	10600	8380	79
2.3	2.25	6360	4060	64
Average		8470	6700	77

Zinc

Figure 6 presents the total and geochemical active concentration of Zn. The highest concentrations are found in the middle layers for both sampling pits. The active fraction is on average a third of the total and varies between 29 and 48% (Table 14). In field soils, the isotopically exchangeable fraction of Zn ranges between 10 and 60 % (Degryse et al., 2009).

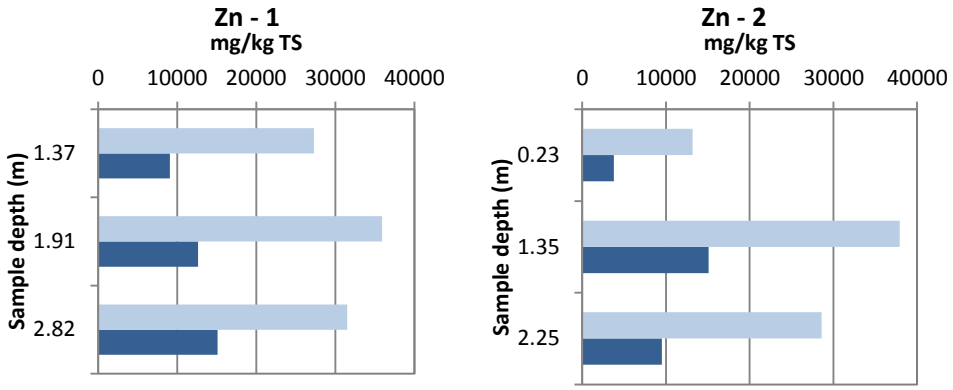

a *b*

Figure 6. Total Zn concentration and concentration extracted with 0.05 M Na_2EDTA for a) *Bergvik 1* and b) *Bergvik 2* at different depths from the surface (m). Total amount based on one sample. Extracted amounts are average values from duplicate samples.

Table 14. *Total and extracted concentration of Zn with 0.05 M Na_2EDTA in mg/kg TS. Extracted concentration also as percentage of the total concentration.*

Sampling points	Depth (m)	TOT mg/kg TS	EDTA mg/kg TS	EDTA % of total
1.1	1.37	27300	9070	33
1.2	1.91	35900	12600	35
1.3	2.82	31500	15100	48
2.1	0.23	13200	3790	29
2.2	1.35	37900	15100	40
2.3	2.25	28600	9500	33
Average		29100	10900	36

Arsenic

The geochemical active fraction of arsenic was in this study represented by the oxalate extractable fraction. In Figure 7 the total concentration and the geochemical active concentration can be seen.

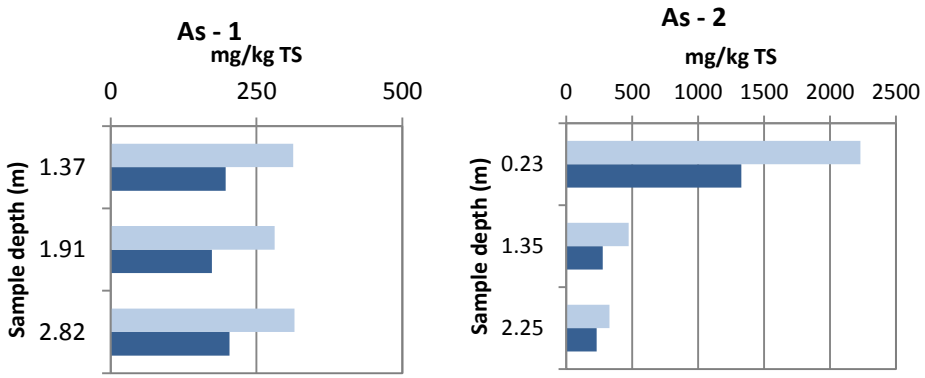

a *b*

Figure 7. Total As concentration and concentration extracted with ammonium oxalate for a) *Bergvik 1* and b) *Bergvik 2* at different depths from the surface (m). Total amount based on one sample. Extracted amounts are average values from duplicate samples. Note the difference in scale between the two figures.

The results differ between and within the two sampling pits. It is especially the uppermost layer of the second sampling pit that distinguishes; with a total concentration of 2230 mg/kg TS compared to concentrations in the range of 281 to 474 mg/kg TS for the rest (Table 15). In the first sampling pit the variation between the layers are quite small but for the second pit a decreasing trend can be seen. The active fraction of arsenic is on average 63 %.

Table 15. *Total and extracted concentration of As with ammonium oxalate in mg/kg TS. Extracted concentration also as percentage of the total concentration.*

Sampling Point	Depth (m)	TOT mg/kg TS	Oxalate mg/kg TS	Oxalate % of total
1.1	1.37	313	197	63
1.2	1.91	281	174	62
1.3	2.82	315	204	65
2.1	0.23	2230	1330	60
2.2	1.35	474	278	59
2.3	2.25	327	232	71
Average		657	402	63

4.2 Solution chemistry

In this section the solution chemistry of the investigated elements are presented and discussed in subsections of natural or pH dependent leaching.

4.2.1 Leaching test at natural pH

In Table 16 the leached concentrations from the tests made on *Bergvik 1:2* and *2:2* at natural pH values are presented. The acceptance criteria (mg/kg at LS 10) for waste to be disposed in landfills are also presented in the Table (NFS 2004:10). The criteria are separated into landfills for inert, non-hazardous or hazardous waste.

Table 16. *Leached concentrations at natural pH for sample 1:2 and 2:2, and criteria for waste to be disposed in landfill for inert, non-hazardous or hazardous waste. Concentrations in mg/kg and valid for an L/S ratio of 10.*

Element	Sample 1:2	Sample 2:2	Inert waste	Non-hazardous waste	Hazardous waste
pH	6.7	6.5			
As	0.14	0.02	0.5	2	25
Cd	1.10	2.74	0.04	1	5
Cu	3.32	1.13	2	50	100
Pb	4.55	3.12	0.5	10	50
Zn	265	539	4	50	200
DOC	47	<5	500	800	1000

The leached concentrations of the elements from the pyrite ash are below the different acceptance criteria for the different classes of landfills. The leached As concentration is below the acceptance criteria for disposal on a landfill for inert waste, Cd below the acceptance criteria for disposal on a landfill for hazardous waste and Cu and Pb below the acceptance criteria for disposal on a landfill for non-

hazardous waste. However, the leached concentration of Zn is too high to be put on a landfill for hazardous waste without pre-treatment. This means that the pyrite ash would have to be stabilised before put on landfill even for hazardous waste.

4.2.2 pH leaching test

The pH dependent leaching of Cd, Cu, Pb, Zn and As are presented in Figure 8-12 for *Bergvik 1:1, 1:3, 2:1* and *2:3.* For the layer *2:1*, the result is presented together with the result from the kinetics study. The total content and geochemical active fraction (EDTA extractable for the cations and ammonium oxalate extractable for As) of the elements are presented in the figures as solid and dashed lines.

The metal cations show strong pH dependency with orders of magnitude changes in solution concentrations. The general pattern is similar for the cations; a maximum concentration at the lowest pH value and a decrease in concentration with increasing pH until around neutral pH (higher for Cd) where a minimum concentration is obtained. At alkaline pH values the concentration starts to increase again for some layers/elements but differences will be further discussed below each Figure. This general pH dependency has been explained by Dijkstra et al. (2009); competition of surface sites with, and a repulsive effect from, protons at low pH values. When the pH increases the surfaces gets more negatively charged which will result in increased sorption and thus decreased concentrations in solution. At alkaline pH values the concentrations in solution increase as a consequence of the formation of inorganic and organic complexes of cations in solution.

For the cations (except for Pb), the amount leached at the lowest pH values correspond well with the EDTA extractable fraction and may indicate that desorption is complete at these pH values. At neutral pH the leached concentration is several orders of magnitude lower than the extracted and total concentration. This indicates that the mechanisms' surface complexation and/or precipitation are of importance in controlling the elements concentration in neutral waters.

Cadmium

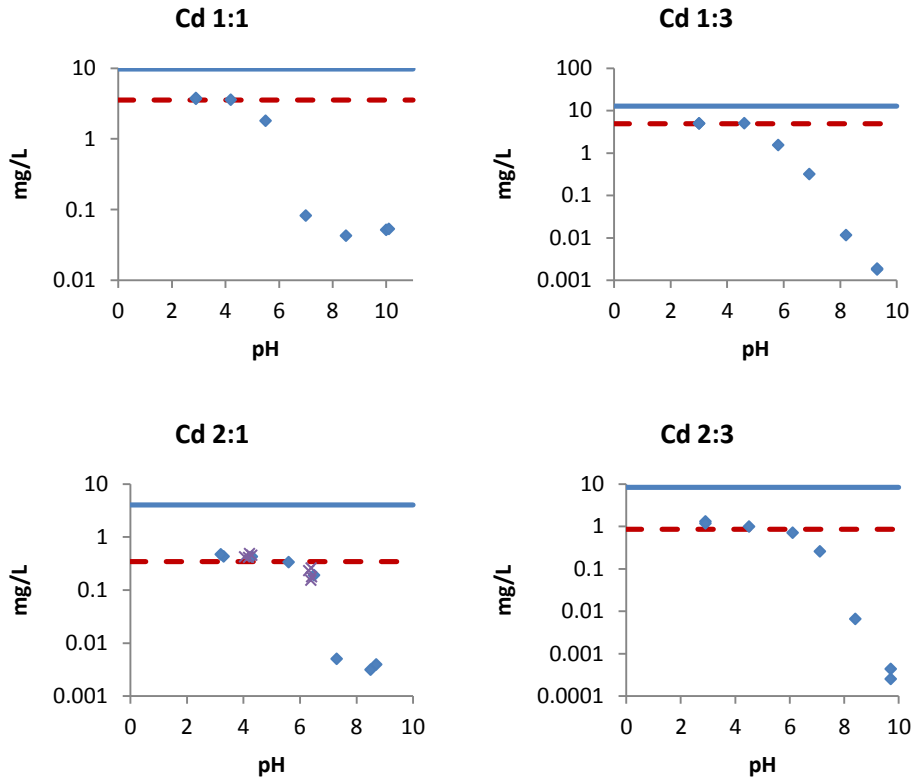

Figure 8. Blue line: total content, red dashed line: amount extracted with 0.05 M Na_2EDTA (recalculated to L/S 10), blue diamonds: concentration leached in pH leaching test, cross: concentration leached in the kinetics study at time 5, 30, 62 and 91 days, for Cd.

If comparing the leached concentration of Cd for the different layers, the overall pattern is similar even though the concentrations differ (Figure 8). As mentioned above, the pH stat concentration at the lower pH values correspond well with the EDTA extractable fraction. Already at pH 4-5 they are similar and desorption seems to be complete. For Cd the dissolved concentration does not increase at alkaline pH values for all layers and where it does, the increase is not very large. The measurements from the kinetics study fit the pH stat curve well.

Copper

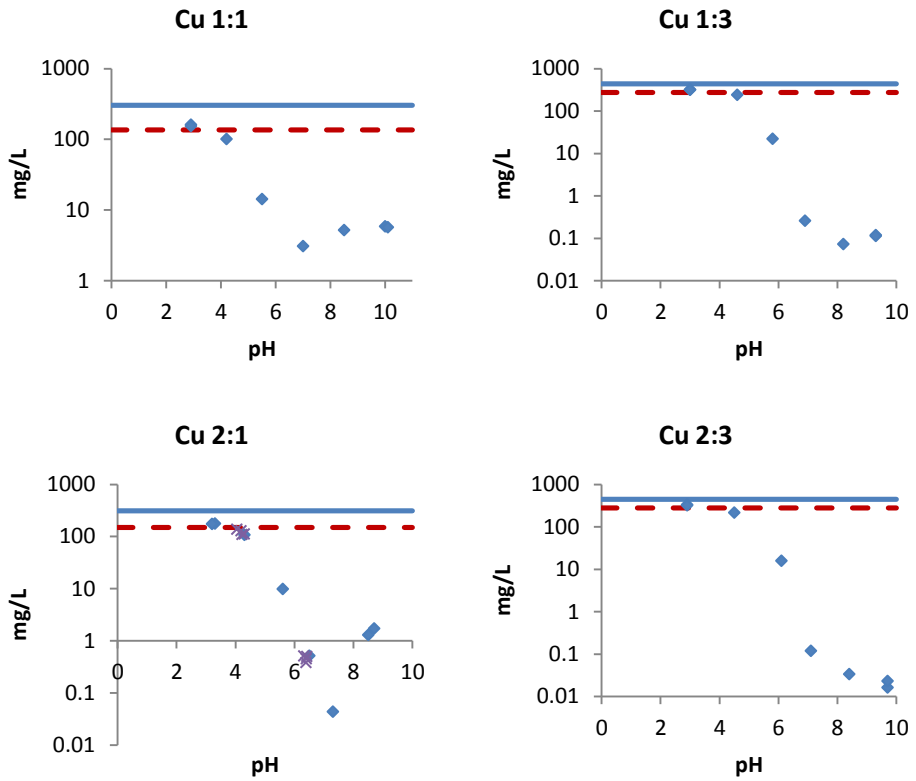

Figure 9. Blue line: total content, red dashed line: amount extracted with 0.05 M Na_2EDTA (recalculated to L/S 10), blue diamonds: concentration leached in pH leaching test, cross: concentration leached in the kinetics study at time 5, 30, 62 and 91 days, for Cu.

The pH-dependent leaching for Cu is similar between the layers and the results from the kinetics study fit the curve well (Figure 9). The EDTA extractable fraction matches the pH stat around pH 3-4 and thus desorption should be complete, if the EDTA correctly estimates the active fraction. For all but one layer (2:3) the concentration starts to increase at alkaline pH values but the increase is not that large for 1:1 and 1:3.

Lead

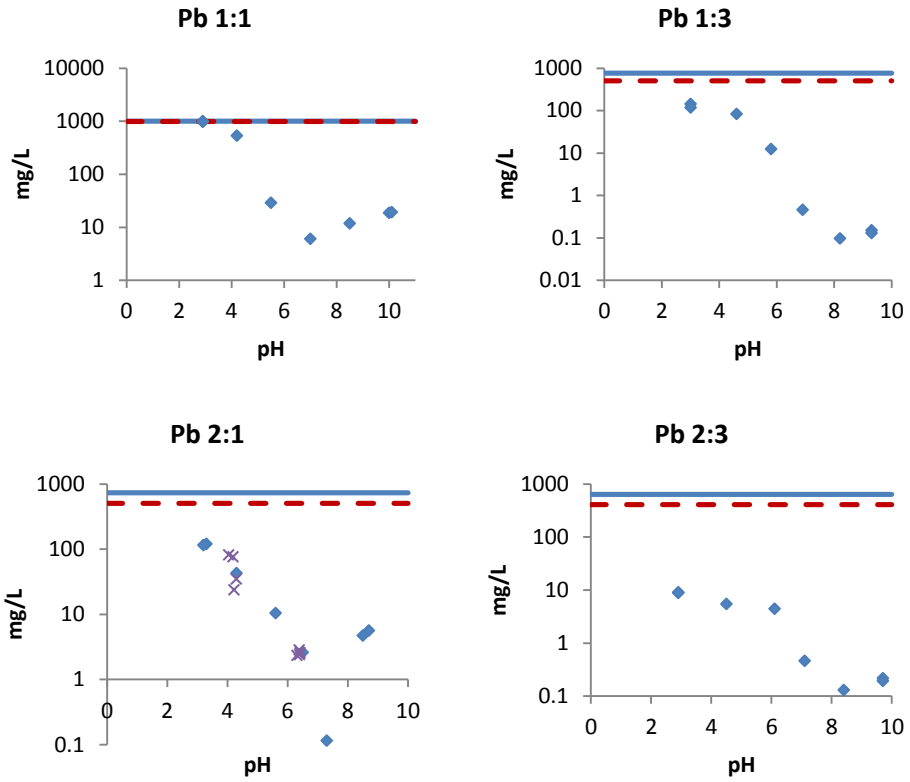

Figure 10. Blue line: total content, red dashed line: amount extracted with 0.05 M Na_2EDTA (recalculated to L/S 10), blue diamonds: concentration leached in pH leaching test, cross: concentration leached in the kinetics study at time 5, 30, 62 and 91 days, for Pb.

For Pb the extractable fraction matches the low pH values in layer 1:1 but not for the others (Figure 10). This could indicate that desorption in these layers is not complete for Pb at the measured pH values. The mismatch is especially pronounced for layer 2:3 where the difference is one order of magnitude. The ferrihydrite concentration in this layer is the second highest (5.09 g/l) but the organic content is the lowest (<0.03 %).

The results from the kinetics study at the lowered pH do not match the form of the pH leaching curve as well as for the other elements. At natural pH however, the results matches well.

Zinc

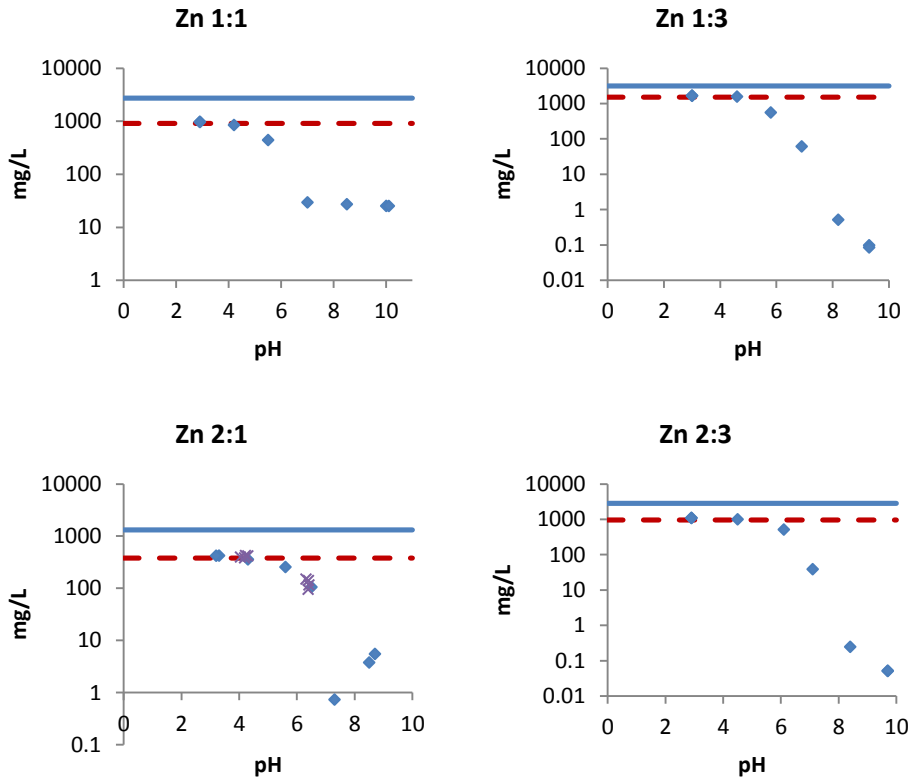

Figure 11. Blue line: total content, red dashed line: amount extracted with 0.05 M Na_2EDTA (recalculated to L/S 10), blue diamonds: concentration leached in pH leaching test, cross: concentration leached in the kinetics study at time 5, 30, 62 and 91 days, for Zn.

If comparing the leached concentration of Zn for the different layers, the pattern is a bit different between different samples (Figure 11). In layer 1:1 the concentration at alkaline pH levels out and for 2:1 it increases. For the deeper layers the concentration continues to decrease. The discrepancy between the layers could be caused by a difference in which mechanism that controls the concentration, if a mineral precipitates at higher pH values or not. Since the concentration increase in layer 2:1 it indicates that soluble complexes are formed and that the concentration is not controlled by a precipitate. For the other layers a precipitate could be the controlling mechanism. The pH stat concentration at pH 4 corresponds well with the EDTA extractable fraction. The measurements from the kinetics study fit the pH stat curve well.

Arsenic

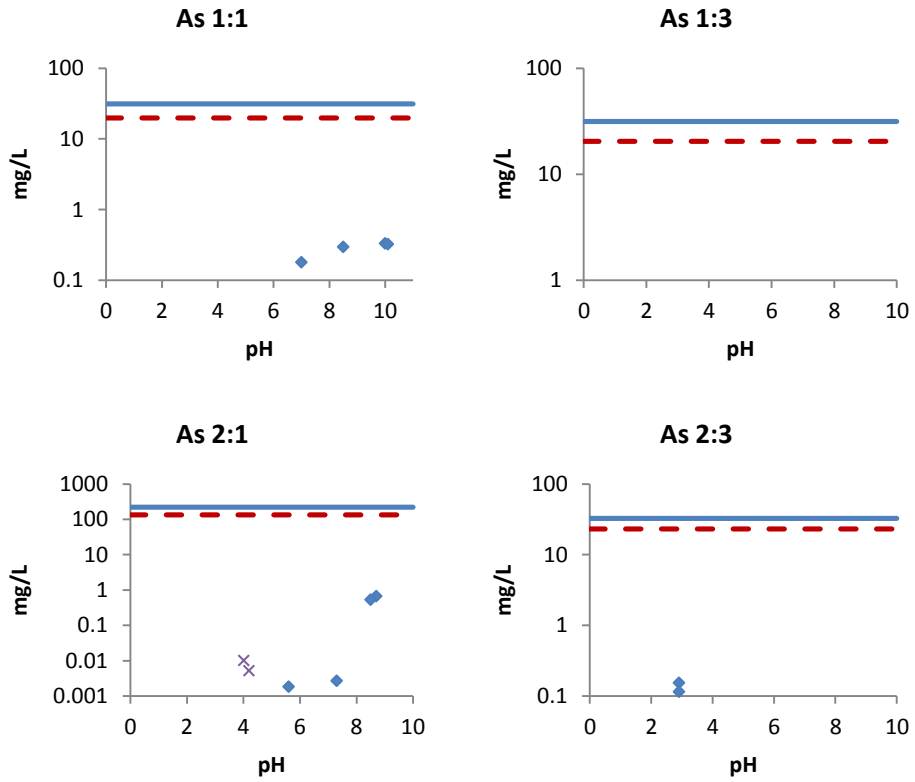

Figure 12. Blue line: total content, red dashed line: amount extracted with 0.05 M Na_2EDTA (recalculated to L/S 10), blue diamonds: concentration leached in pH leaching test, cross: concentration leached in the kinetics study at time 5, 30, 62 and 91 days, for Zn.

Many of the obtained results for As from the pH leaching test were below detection limit and not presented in the Figure (Figure 12). The pH dependency for As is therefore not easily seen. From the kinetics study, results above the detection limit was attained for two more pH values and the minimum concentration for As seem to be located at pH around 5.5. For As the amount leached in the pH leaching test around neutral pH is much less than the extracted amount indicating that surface complexation or precipitation control the concentration of As in solution.

4.2.3 Kinetics

The effect of time on reaction development was investigated in the kinetics study. As mentioned in the previous section the results from the kinetics study, for all elements but Pb, matched the curve of the pH dependent leaching quite well. However, the pH-dependent measurements were presented as their logarithmic values and small changes are therefore not easily seen.

In Figure 13 the leached concentration of Cd, Zn, Cu and Pb are plotted as a function of time. The results for As are not presented in a Figure since there were only two results above detection limit.

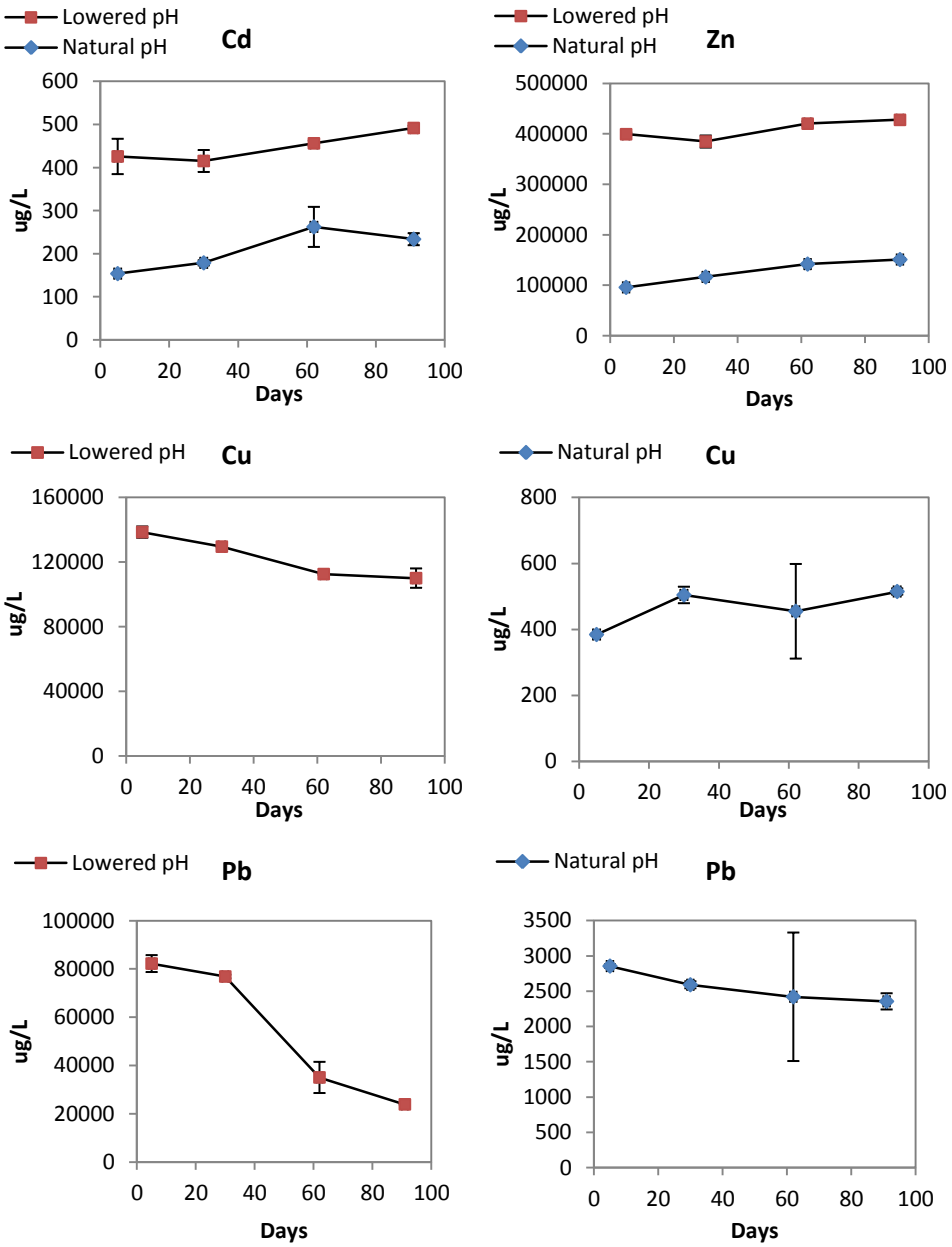

Figure 13. Leached concentration of Cd, Zn, Cu and Pb (ug/l) as a function of time (days). Red squares: Lowered pH and blue diamonds: natural pH. Average values of duplicate, error bars represent one standard deviation in both directions.

No statistics have been made on the results since there are too few measurements. Too get reliable statistics over reaction development, a longer time period or a higher sampling frequency is needed. However, from the results above it seems like the leached concentrations of Cd and Zn are increasing with time for both the lowered and natural pH but the change is not that large. For Cu (only the lowered pH) and Pb the form of the curve is downwards and indicates a decreasing concentration in solution. Figure 14 presents the change in pH with time for both the samples with natural and a lowered pH.

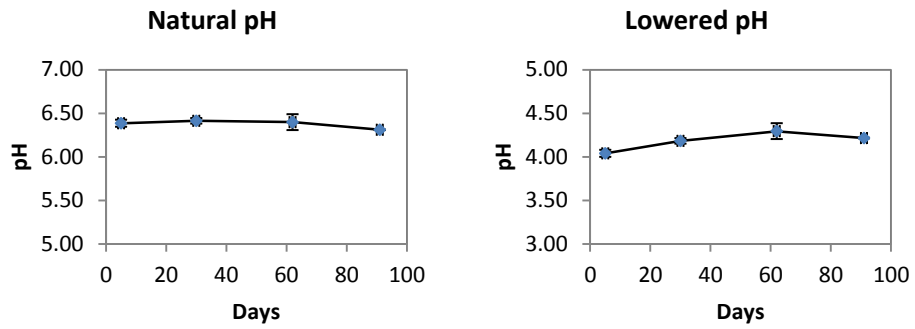

Figure 14. pH plotted against days. Average values of duplicate samples, error bars represent one standard deviation in both directions. Note the difference in scale between the two figures.

Only small changes in pH can be seen and to evaluate if they were of importance for the changed concentrations, the pH was plotted against the concentrations measured at the different time intervals (Figure 15).

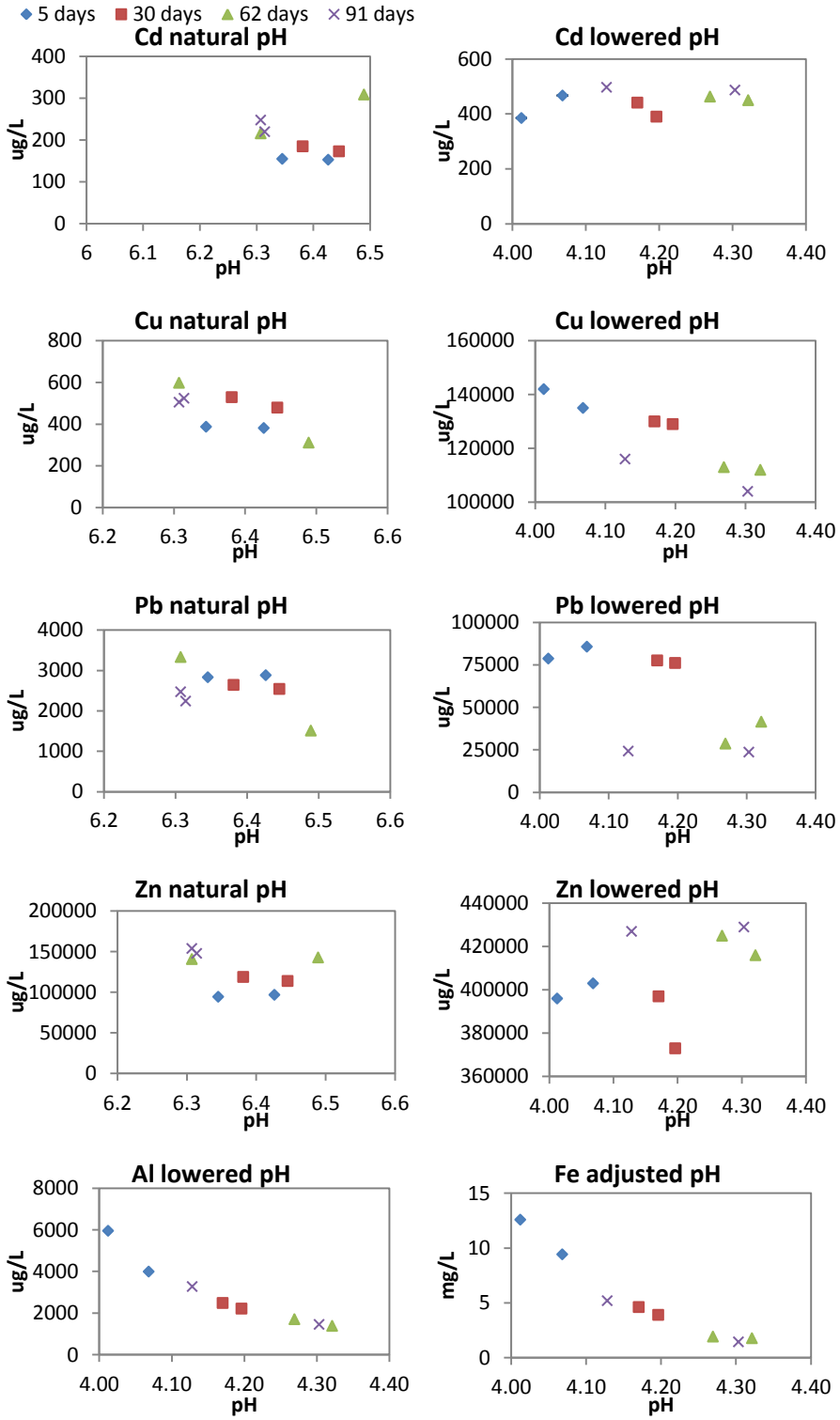

Figure 15. Measured concentrations from the kinetics study after 5, 30, 62 and 91 days against pH.

There is no clear relationship between concentration and pH for Cd and Zn. For Cu and Pb the decreasing concentrations seem to be correlated to an increase in pH. More samples are however needed to better relate the changed concentration to the change in pH. For Al and Fe there is a clear relationship between decreasing concentrations and increasing pH.

In Figure 16 the sulphate concentrations obtained in the pH leaching test and from the kinetics study (measured after 91 days) are plotted against pH. An increased sulphate concentration with time could indicate that residues of pyrite in the ash are being oxidised (Nordbäck, et al., 2004a). When pyrite is oxidised, Fe^{2+} and SO_4^{2-} is released together with protons and the pH is lowered. Lowered pH could then lead to increased leaching of metals from the ash.

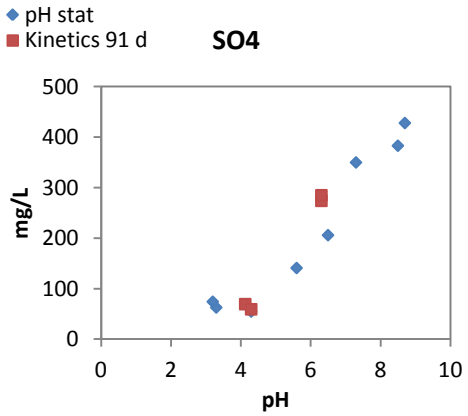

Figure 16. Sulphate concentration plotted against pH. Red squares: results from kinetics study after 91 days, blue diamonds: pH dependent leaching test. Tests performed on *Bergvik 2:1* at an L/S of 10.

The sulphate concentrations from the kinetics study are following the pH leaching curve quite well. Thus, the result indicates a low content of reactive sulphides in the sample.

Figure 17 presents both the DOC concentration as a function of time and pH. The results from the last measurement at 91 days were below detection limit (5 mg/L, higher limit due to small sample volume) and are represented with open symbols.

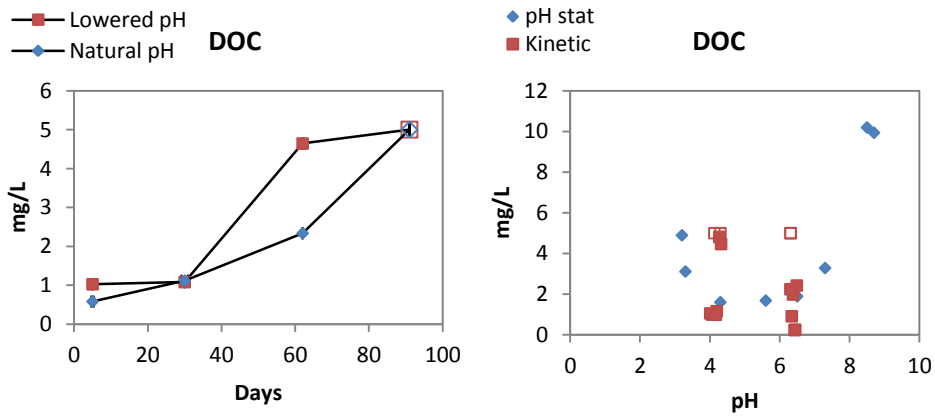

a *b*

Figure 17. DOC concentration plotted against a) days and b) pH. Open symbols represents the detection limit for the values obtained from the last measurement (91 days) since they were below the limit. a) Average values of duplicate, error bars represent one standard deviation in both directions.

It seems like the DOC concentration is increasing with time for both lowered and natural pH. The kinetics results are also not following the form of the pH leaching curve. Since Pb and Cu are strongly associated with organic matter, it is surprising that the two metals do not follow the same pattern as the DOC concentration. If organic matter is dissolved, Pb and Cu attached to the OM should be realeased. However, since Pb and Cu also have got high affinity for binding to oxide surfaces they may compete with other elements for the reactive sites of the oxide surfaces. This could be the explanation to the increased concentrations of Cd and Zn in solution, since they are not bidning as strongly as Pb and Cu.

4.3 Geochemical modelling

4.3.1 Solution speciation

Natural pH

Figure 18 presents the species distribution calculated with VM of the metal cations Cd, Cu, Pb and Zn and the anion As in the leachate from the water leaching test with natural pH. The species are free dissolved, bound to inorganic ligands or bound to dissolved organic matter. The water leaching test was made on sample *Bergvik 1:2* with a pH-value of 6.7 in the leachate and on *Bergvik 2:2* with a pH-value of 6.6 in the leachate.

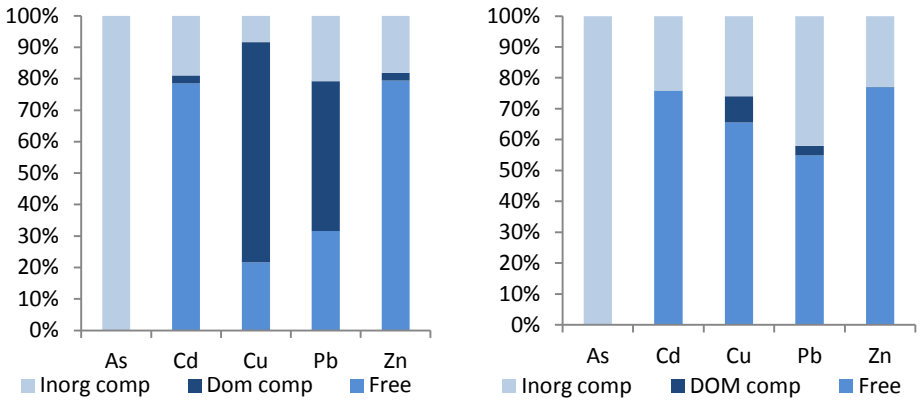

Figure 18. Predicted speciation distribution in the leachate from the water leaching tests made on a) *Bergvik 1:2* and b) *2:2*. Average values from duplicate samples.

The dominant form of Cd and Zn is the dissolved free ion. Of the total dissolved, the free Cd ions constitute 78% in sample 1:2 and 76% in sample 2:2. For Zn the free ions constitute 79% in sample 1:2 and 77 % in sample 2:2.

Arsenic is exclusively found as inorganic complexes, as the species $HAsO_4^{2-}$ and $H_2AsO_4^-$. Cu and Pb have a higher affinity for binding to organic matter, however the variation between the two sampling points is quite large. This can be explained by the low concentration DOC in sampling point 2:2. The reported concentration of DOC was below the detection limit and was set to 0.25 mg/L, which was half the detection value. The concentration DOC in layer 1:2 was 4.7 mg/L (average from duplicate samples).

pH dependent speciation

In Figure 19 the predicted pH dependent speciation for Cd, Cu, Pb, Zn and As with VM is presented.

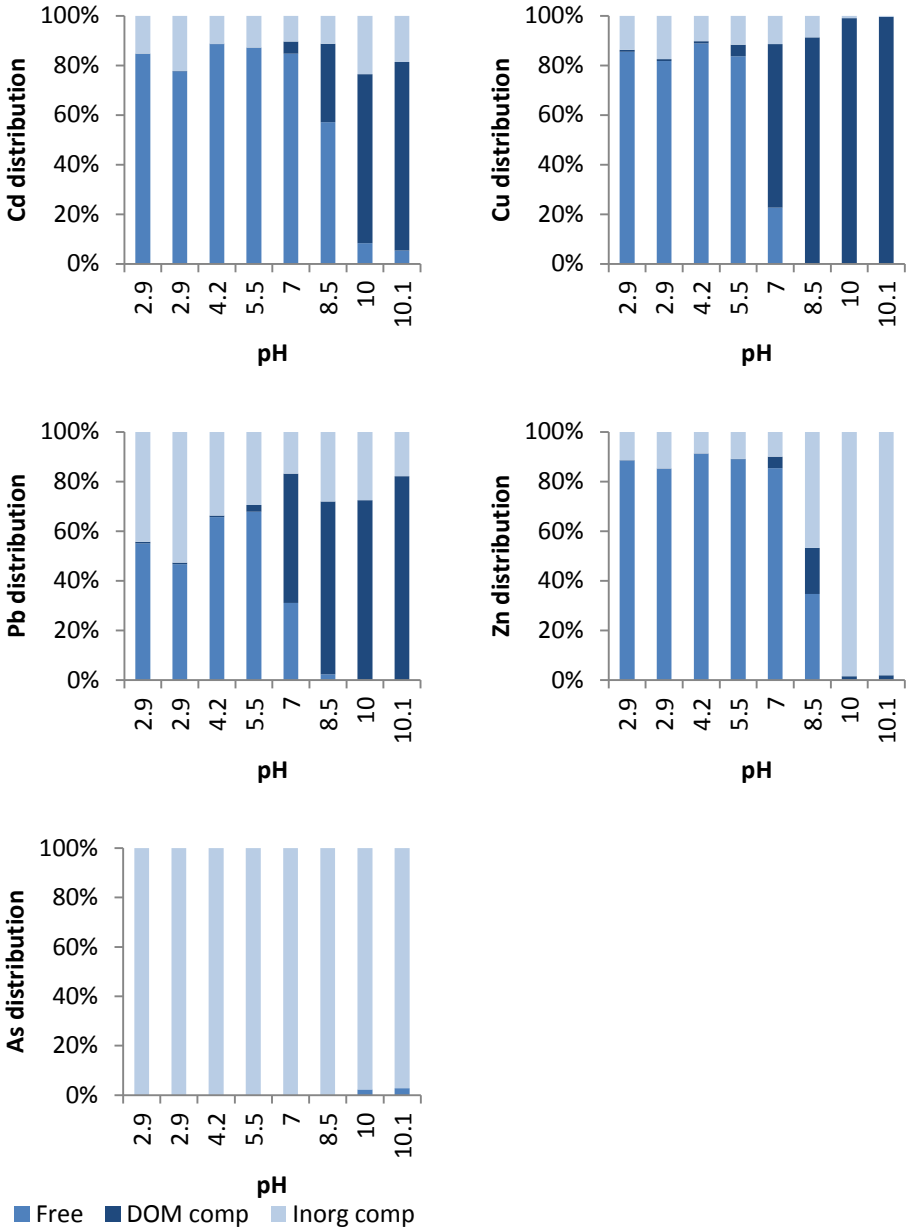

Figure 19. Predicted speciation distribution for *Bergvik 1:1* plotted against pH.

The metal cations show similar trends; the free ion concentration dominate at low pH values and the complexes with DOM get more pronounced at higher pH values. The free form dominates up to around pH 8.5 for Cd, pH 7 for Zn and pH 5.5 for Pb and Cu.

For Zn the inorganic complexes are more important than the organic complexes at alkaline pH values where this form dominates. The higher affinity of Cu and Pb

for organic matter are also easily seen; compared to Cd and Zn they bind to DOM at lower pH values and with a greater fraction. The DOM complexes are the dominant form for Cu and Pb at neutral and alkaline pH values. They are also the dominant form for Cd at pH values above 10.

For As the inorganic complexes are dominant throughout the whole pH range.

4.3.2 Solubility control mechanisms

The saturation indices (SI) provide information about important minerals controlling the free metal ion concentration. The minerals close to equilibrium (-1 <SI> 1) are of interest. When modelling the results from the pH leaching test, indications of controlling minerals could be seen for zinc, copper and aluminium and in some cases for lead. However, the different sampling points gave slightly different results. Important mineral phases, their reactions and solubility constants can be seen in Table 17.

Table 17. *Important mineral phases, their reactions and their solubility constants (from VM database).*

Mineral	Chemical reaction	log K_s (20 °C)
$Al(OH)_3$ (soil)	$Al(OH)_3$ (soil) + 3 $H^+ \leftrightarrow Al^{3+}$ + 3 H_2O	8.29
Ferrihydrite	$Fe(OH)_3 + 3H^+ \leftrightarrow Fe^{3+}$ + 3 H_2O	3.2
Tenorite, cristal.	CuO (s) + $2H^+ \leftrightarrow Cu^{2+}$ + H_2O	7.64
$Cu(OH)_2$ (s)	$Cu(OH)_2$ (s) + $2H^+ \leftrightarrow Cu^{2+}$ + 2 H_2O	9.29
$Pb(OH)_2$ (s)	$Pb(OH)_2$(s) + $2H^+ \leftrightarrow Pb^{2+}$+ + 2 H_2O	8.15
Cerrusite	$PbCO_3$ (s) $^+ \leftrightarrow Pb^{2+}$ + CO_3^{2-}	-13.2
Zincite	ZnO + 2 H+ $\leftrightarrow Zn^{2+}$ + H_2O	11.23
$Zn(OH)_2$ (epsilon)	$Zn(OH)_2$ (s) + $2H^+ \leftrightarrow Zn^{2+}$ + 2 H_2O	11.534

The minerals presented in Table 17 were further investigated in VM by adding them as possible solids. Adding the minerals $Al(OH)_3$ (soil), $Zn(OH)_2$ (epsilon) and tenorite (cr.) gave the model output a better fit to the experimental data. Figure 20-22 present saturation indices plotted against pH for these minerals.

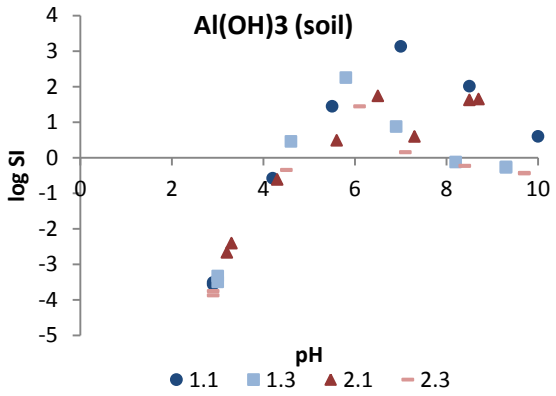

Figure 20. Saturation index for $Al(OH)_3$ (soil) for layer 1:1, 1:3, 2:1 and 2:3 plotted against pH. pH of natural samples are in the range 6.5 – 7.1.

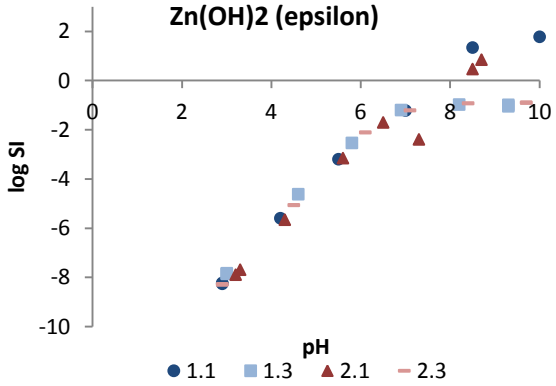

Figure 21. Saturation index for Zn(OH) (epsilon) for layer 1:1, 1:3, 2:1 and 2:3 plotted against pH. pH of natural samples are in the range 6.5 – 7.1.

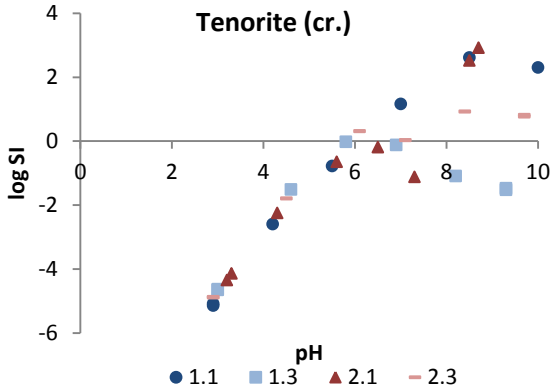

Figure 22. Saturation index for tenorite (crystalline) for layer 1:1, 1:3, 2:1 and 2:3 plotted against pH. pH of natural samples are in the range 6.5 – 7.1.

The aluminium hydroxide seems to be important at pH values above 4 where it is supersaturated. If adding the mineral as a possible solid in the surface complexation model, it will most probably control the Al concentration above this pH.

The zinc hydroxide and the copper oxide (tenorite) are also at higher pH values supersaturated and may control the free ion concentrations of Zn and Cu by precipitation. For Zn precipitation seems to be important at pH values above 8 and for Cu at pH values above 6. Precipitation of a copper mineral could thus be important at natural pH values, which were in the range 6.5 – 7.1 for the layers investigated in VM.

For Cd and As, which did not seem to have a mineral phase controlling the concentration of the element in solution, surface complexation is probably the controlling process.

Cerrusite, a lead carbonate mineral, was also supersaturated (in the surface layers) with respect to the concentrations of the elements at high pH values (Figure 23). However, it did not seem to improve the fit of the model and was therefore not added in the surface complexation modelling.

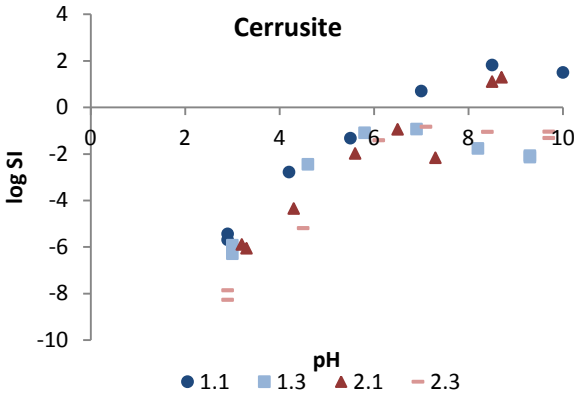

Figure 23. Saturation index for cerrusite for layer 1:1, 1:3, 2:1 and 2:3 plotted against pH. pH of natural samples are in the range 6.5 – 7.1.

4.3.3 Surface complexation modelling

In VM also surface adsorption to SOM and to oxides can be modelled. As mentioned in the method section, the estimated ferrihydrite concentration from the oxalate extraction (see Table 9), and the estimated concentration of fulvic and humic acid from the TOC concentration, were used as input in the surface models.

Since the modelling was working better if one of the two surface models; solid organic matter or surface complexation reactions, was excluded, it was investigated which of the two models alone that gave the lowest concentrations of Cd, Cu, Pb Zn and As in solution (for sample 1:1). This would thus indicate that this

surface model played a greater role in controlling the element's concentrations. As can be seen in Figure 24 the surface complexation model with ferrihydrite (HFO model) gave lower than, or similar to, the concentrations predicted by the soil organic matter model (SOM model) using Stockholm Humic Model, for all elements and in the whole pH range.

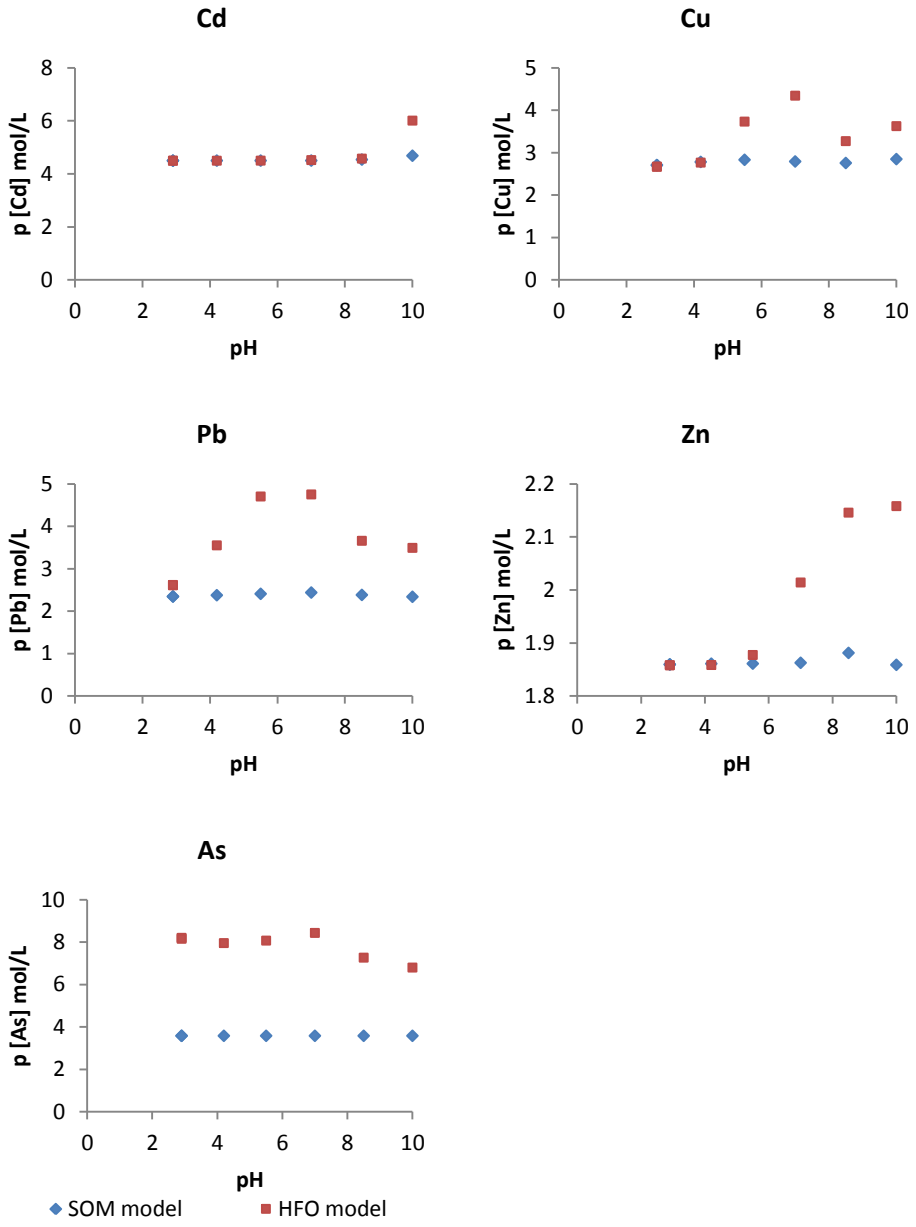

Figure 24. Total dissolved concentration in mol/L of Cd, Cu, Pb, Zn and As predicted with VM using either blue diamonds: sorption to soil organic matter or red squares: sorption to (hydr)-oxide surfaces. Note that the concentrations are in their minus logarithm (p) values. Comparison made on sample 1:1.

For Cd, Cu and Zn the predicted concentrations with the HFO model were similar to the concentrations predicted with the SOM model at low pH values (all but the highest for Cd), and thus indicated that sorption to organic matter at these pH values could be at least as important (or unimportant) as sorption to (hydr)oxide surfaces. However, since the concentrations are in the same magnitude, the use of the HFO model alone should be able to do reliable estimates of the concentrations. The distribution between sorption sites may on the other hand not be correctly predicted. The modelling was proceeded with only sorption to oxide surfaces and the solid organic matter model was left out. The model comparison was conducted on layer 1:1, which had the second lowest concentration of ferrihydrite (5.01 g/l) and the highest content of solid organic matter (1.11 g/l) of the layers. This simplification should therefore be valid also for the other layers.

4.3.4 Comparison predicted and measured concentrations

The differences observed for the *predicted* pH dependent leaching between the different sampling points, can be explained by the difference in amount of reactive surfaces and geochemical active fraction of the contaminants that have been used as input in the model. The model is described in the section 3.3.3 and in Table 5.

Aluminium

Figure 25 presents the total dissolved concentration of Al predicted by the model and from the pH leaching test.

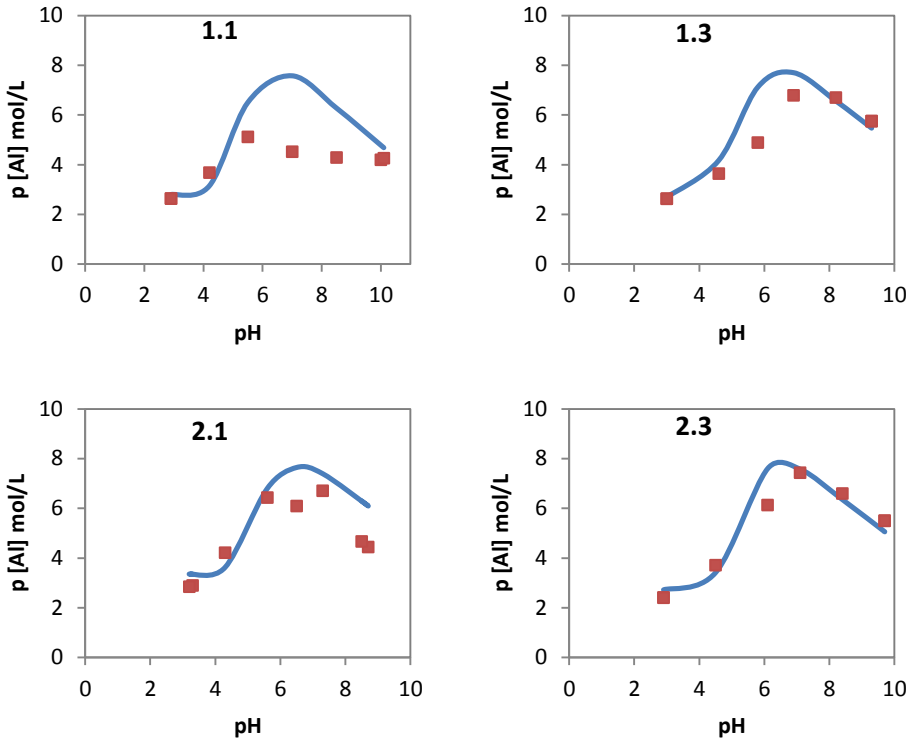

Figure 25. Total dissolved concentration of Al for layer 1:1, 1:3, 2:1 and 2:3 in mol/L plotted against pH. Blue line: model simulation, red squares: measurements from pH leaching test. Note that the concentrations are in their minus logarithm (p) values.

Generally, the Al concentrations are correctly predicted over the whole pH range but for layer 1:1 the predicted concentrations are underestimated up to 3 orders of magnitude in the pH interval 5-9.

The distribution details derived from the model output (Figure 26) show that the model predict that the activity of aluminium is highly controlled by precipitation of $Al(OH)_3$ (soil) at pH above 4.

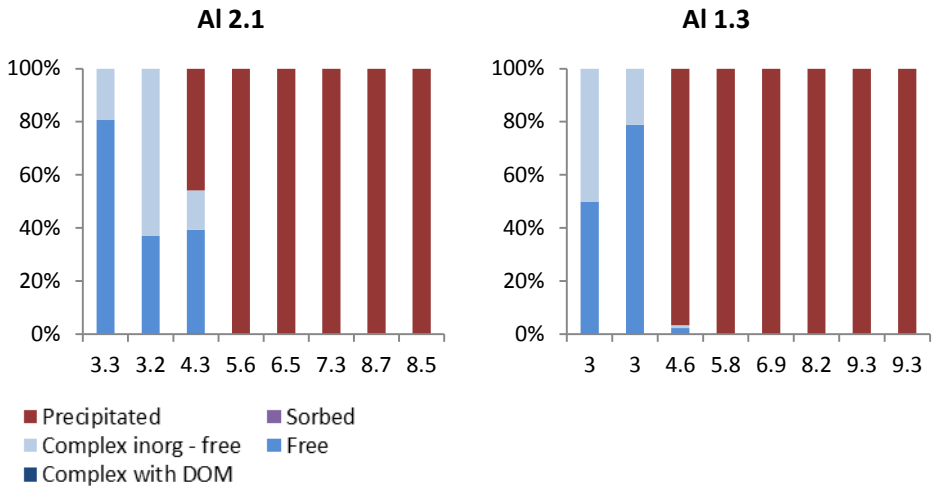

Figure 26. Predicted distribution of Al ions. Note that the SOM model was excluded. The measured natural pH was 6.5 for layer 2.1 and 6.9 for layer 1.3.

The species distribution is only presented for two layers and they were chosen according to their estimated ferrihydrite concentration. Layer 2.1 had the highest estimated concentration (6.93 g/l) and layer 1.3 had the lowest estimated concentration (4.36 g/l) of ferrihydrite. The measured natural pH was 6.5 for layer 2.1 and 6.9 for layer 1.3

Iron

Figure 27 present the dissolved concentration of Fe derived from the model and the pH leaching test. The mineral ferrihydrite (am) was set to control the concentration of iron in solution. This is an iron oxide with high solubility, yet the concentration in solution is underestimated for all sampling points. This could be an indication that the measured iron concentration includes more than the dissolved form, and that colloids of iron passes through the filters used in the experiments. Regelink et al. (2014) found iron (hydr)oxide colloids as small as 2-5 nm in their filtrated solution. These iron colloids have high sorptive capacity and may play a great role in binding trace metals in the soil-solution and enhance their mobility.

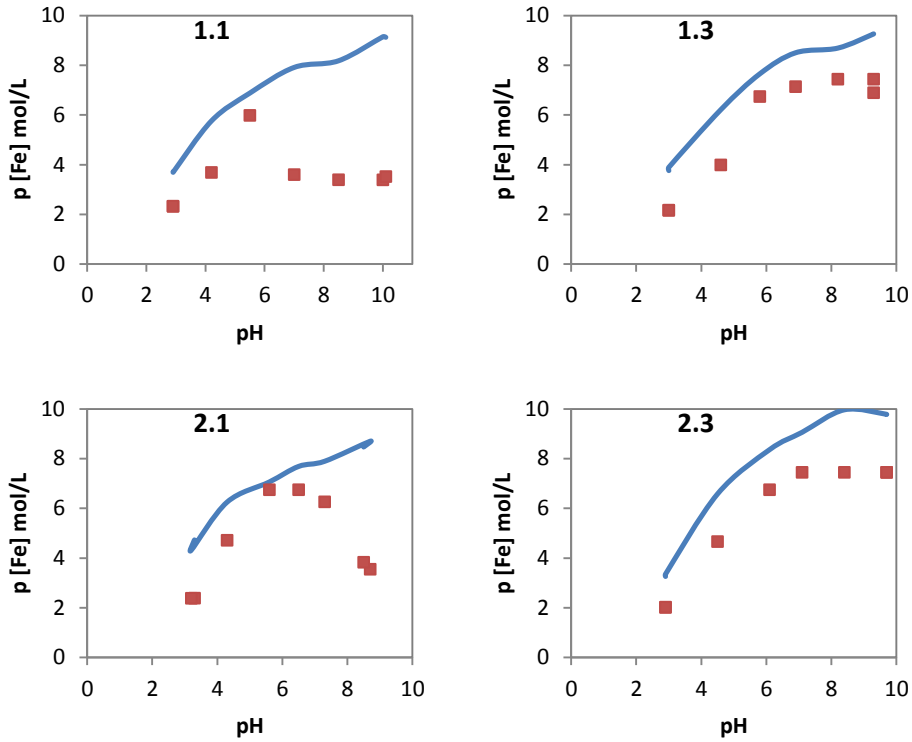

Figure 27. Total dissolved concentration of Fe for layer 1:1, 1:3, 2:1 and 2:3 in mol/L plotted against pH. Blue line: model simulation, red squares: measurements from pH leaching test. Note that the concentrations are in their minus logarithm (p) values.

Cadmium

The shape of the model curve for Cd match the experimental data quite well and the model's estimate of the dissolved concentration can be considered reasonable (Figure 28). In the Figure also the predicted solution concentration without any possible solids for Cu and Zn are presented (dashed line).

When calibrating the model, it was obvious that the Cd concentration was highly affected by precipitations of minerals containing zinc and copper. If solids including zinc or copper were allowed to precipitate, the concentration of cadmium matched the experimental concentrations better. Competition of surface sites may be the explanation to this effect. Since cadmium is binding more weakly in the soil than Cu and Zn, competition of surface sites may result in less binding of Cd when ions of Cu and Zn are present. If the concentrations of Zn and Cu are controlled by precipitation of minerals, their dissolved concentrations, and the competition with Cd, will be less. The concentration of Cd in solution is thus controlled by adsorption and desorption from oxide surfaces but highly dependent on concentration of other competing ions.

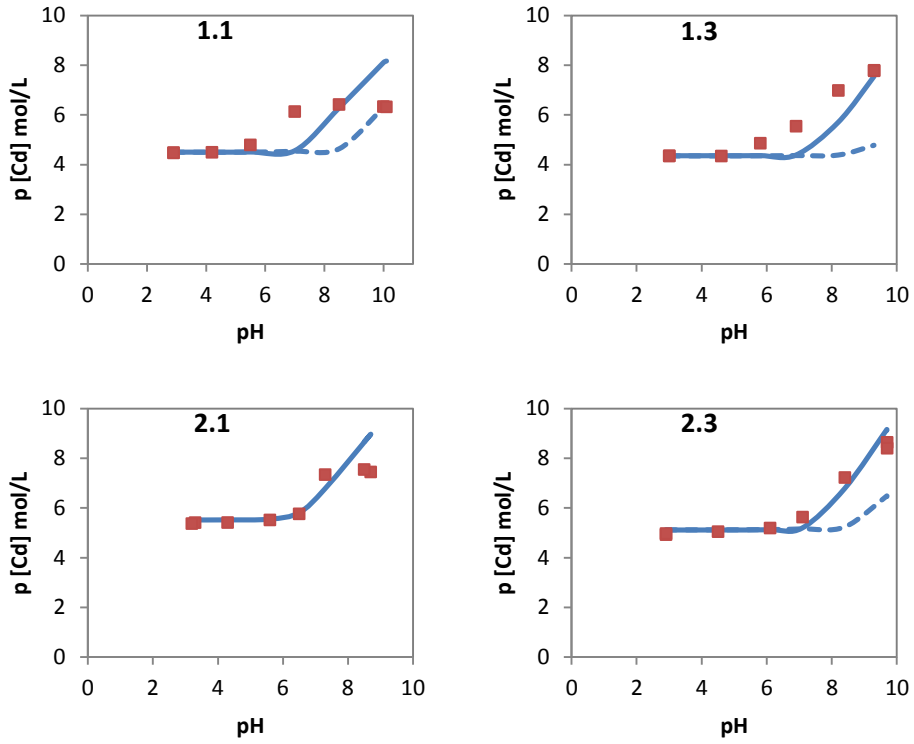

Figure 28. Total dissolved concentration of Cd for layer 1:1, 1:3, 2:1 and 2:3 in mol/L plotted against pH. Blue solid line: model simulation, blue dashed line: model simulation without possible solids for Cu and Zn, red squares: measurements from pH leaching test. Note that the concentrations are in their minus logarithm (p) values.

The species distribution predicted by the model (Figure 29) shows that the free dissolved form is dominant until approximately natural pH. At alkaline pH values almost all Cd is sorbed to (hydr)oxide surfaces.

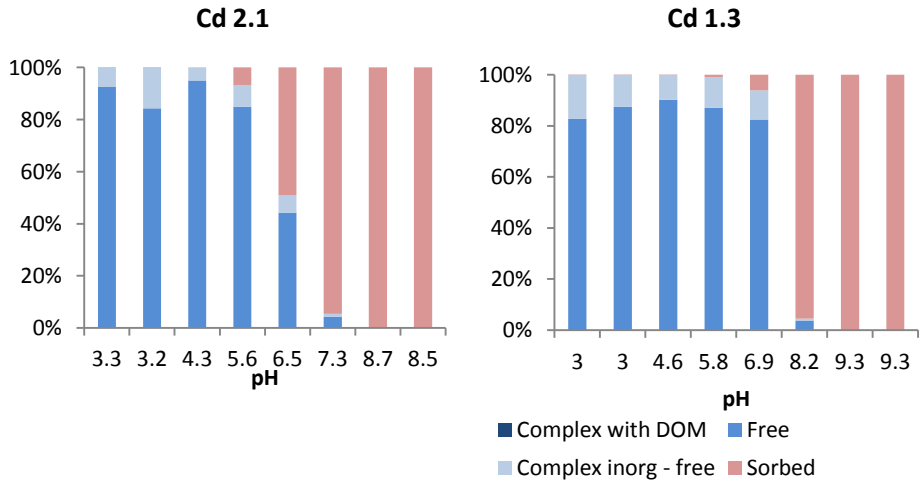

Figure 29. Predicted distribution of Cd ions. Note that the SOM model was excluded. The measured natural pH was 6.5 for layer 2.1 and 6.9 for layer 1.3.

Copper

The Cu concentration predicted from the model also matches the experimental data quite well (Figure 30).

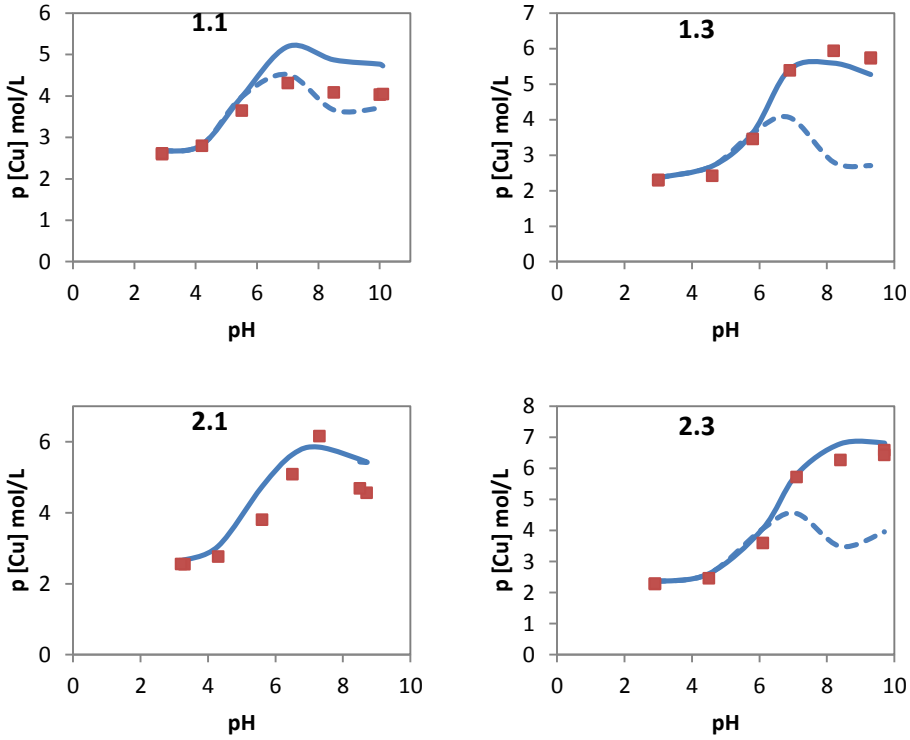

Figure 30. Total dissolved concentration of Cu for layer 1:1, 1:3, 2:1 and 2:3 in mol/L plotted against pH. Blue solid line: model simulation, blue dashed line: model simulation without possible solids for Cu and Zn, red squares: measurements from pH leaching test. Note that the concentrations are in their minus logarithm (p) values.

For layer 1.1 the model predicts the concentration better if no possible solids for Cu or Zn are added, but for 1.3 and 2.3 a better fit can be seen if solids are allowed to precipitate. However, even if the copper mineral tenorite is added as a possible solid for layer 2.1, it do not precipitate (Figure 31). The content of ferrihydrite in this layer is higher and the concentration of copper is lower compared to other layers. High sorption of Cu to oxide surfaces and low concentration of Cu in solution result in to low ion activity product and therefore no mineral will precipitate. For layers with less oxide surfaces and higher geochemical active Cu concentrations as input, the mineral tenorite precipitates. At natural pH surface complexation is the controlling mechanism for layer 2.1 whereas it is precipitation for layer 1.3.

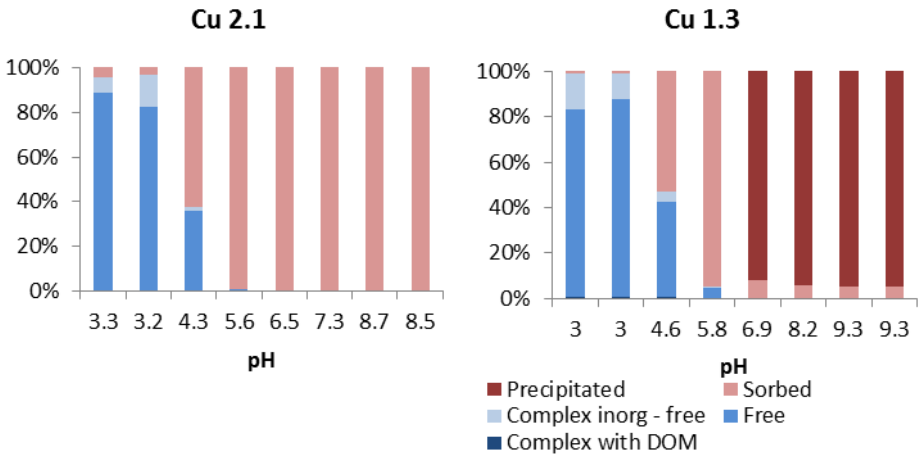

Figure 31. Predicted distribution of Cu ions. Note that the SOM model was excluded. The measured natural pH was 6.5 for layer 2.1 and 6.9 for layer 1.3.

Lead

The predicted Pb concentration (Figure 32) does not match the measured data as well as the model for Cd and Cu. The Pb concentration at high pH is also affected by precipitation of Zn- and Cu minerals.

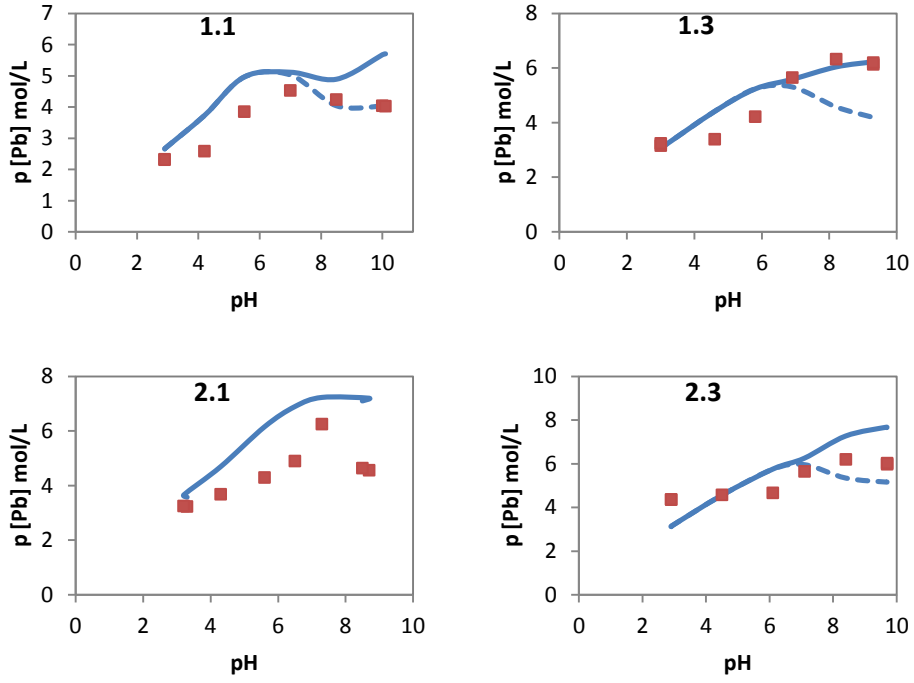

Figure 32. Total dissolved concentration of Pb for layer 1:1, 1:3, 2:1 and 2:3 in mol/L plotted against pH. Blue solid line: model simulation, blue dashed line: model simulation without possible solids for Cu and Zn, red squares: measurements from pH leaching test. Note that the concentrations are in their minus logarithm (p) values.

The concentration of Pb in solution is under estimated for most layers and pH values but for the lowest pH value in layer 2.3 the concentration in solution is overestimated. As mentioned previously, the EDTA extractable fraction for this layer did not match the measured concentration at the lower pH values. The EDTA extractable concentration can therefore for this layer be assumed to be overestimated. At higher pH values the concentration is on the other hand underestimated as for the rest of the layers.

The reason for this underestimation predicted by the model could be the same as with the iron concentration; colloidal particles of lead in the measured solution. Lead has shown to have high affinity for binding to colloid iron (hydr)-oxides and since it is assumed that they are present in the solution, it is highly possible that they are affecting the mobilisation of lead (Pédrot et al., 2008).

From the predicted distribution (Figure 33) it is obvious that sorption to oxide surfaces is an important process and already at pH values around 3. Since the sorption is that important, the estimated concentration of active surfaces has a large effect on the concentration of Pb in solution.

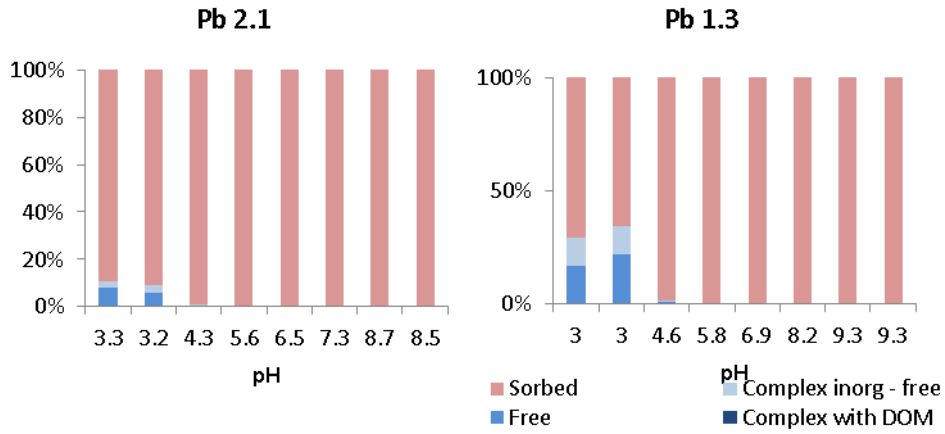

Figure 33. Predicted distribution of Pb ions. Note that the SOM model was excluded. The measured natural pH was 6.5 for layer 2.1 and 6.9 for layer 1.3.

Zinc

The predicted concentration of Zn is reasonably well estimated for all layers and pH values, except for higher pH values in layer 1.1 (Figure 34). The added mineral zinc hydroxide precipitates at alkaline pH values, but as previously discussed for Cu, the mineral does not precipitate in layer 2.1 where the ferrihydrite concentration is higher (Figure 35). At natural pH, Zn adsorbed to ferrihydrite dominates the solid-solution partitioning for layer 2.1, and the free hydrated species dominate in layer 1.3.

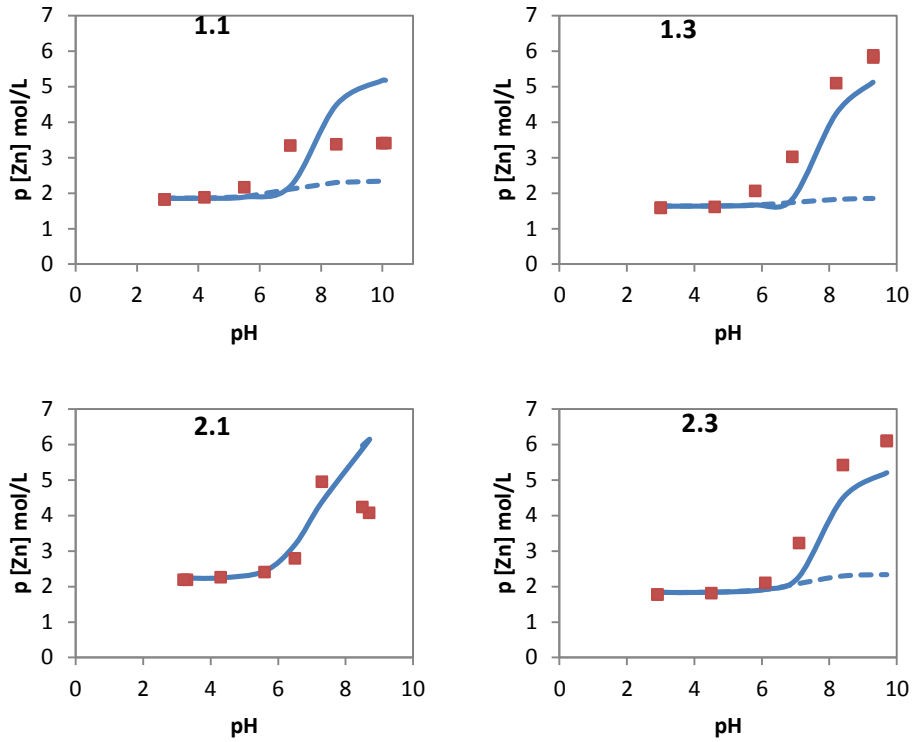

Figure 34. Total dissolved concentration of Zn for layer 1:1, 1:3, 2:1 and 2:3 in mol/L plotted against pH. Blue solid line: model simulation, blue dashed line: model simulation without possible solids for Cu and Zn, red squares: measurements from pH leaching test. Note that the concentrations are in their minus logarithm (p) values.

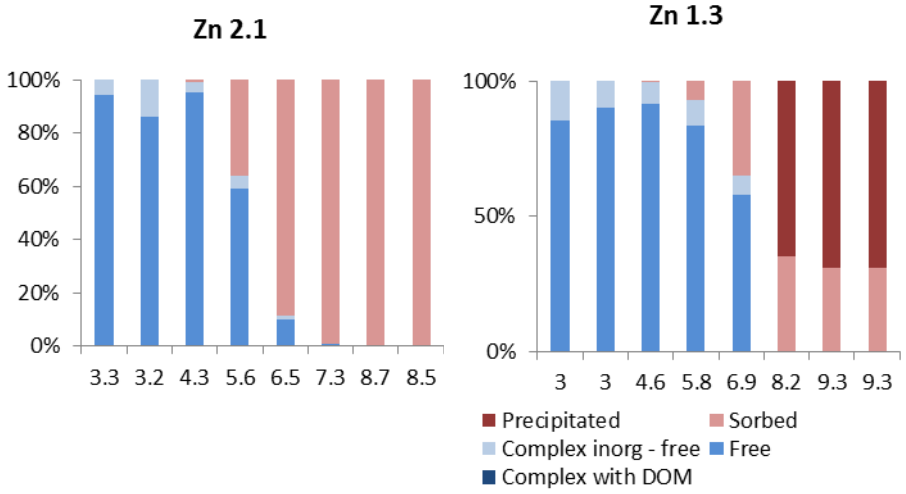

Figure 35. Predicted distribution of Zn ions. Note that the SOM model was excluded. The measured natural pH was 6.5 for layer 2.1 and 6.9 for layer 1.3.

Arsenic

For arsenic the concentration is controlled by adsorption to oxide surfaces over the whole pH range. As seen in Figure 36 the predicted concentration is hardly affected by a change in pH. The amount of oxide surfaces seem to be more than enough for adsorbing As ions, even at high pH values where the surface gets more negatively charged. The result from the model is hard to verify due to too few measurements, but it seems like the model underestimates the As solution concentration. The concentration of As in solution is affected by precipitates of Zn- and Cu minerals. Lower As concentration in solution can be seen when the minerals are allowed to precipitate, and therefore it can be concluded that also As is competing for reactive surfaces with the cations.

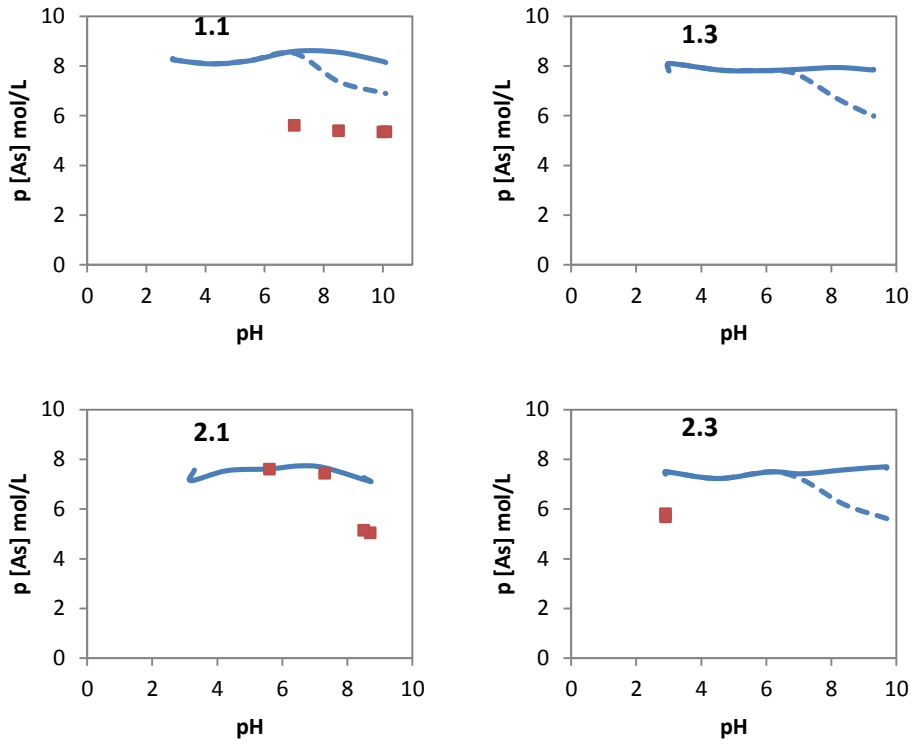

Figure 36. Total dissolved concentration of As for layer 1:1, 1:3, 2:1 and 2:3 in mol/L plotted against pH. Blue line: model simulation, red squares: measurements from pH leaching test, blue dashed line: model simulation without possible solids for Cu and Zn, red squares: measurements from pH leaching test. Note that the concentrations are in their minus logarithm (p) values.

5 Conclusions

In this thesis the geochemistry of pyrite ash have been investigated with the use of selective extraction methods, leaching tests and geochemical modelling. The water leaching tests illustrate that if the pyrite ash was produced today it would be classified as hazardous waste that would need to be stabilised before put on a landfill. It is in other words a severe soil contaminant and sites contaminated with pyrite ash should be assessed regarding the risk it poses to humans and the environment.

The metal cations showed strong pH dependency with high solution concentrations at low pH values. The leached concentration at the lowest pH values corresponded well with the Na_2EDTA extractable fraction for all metals, except for lead at some sampling points, but at neutral pH the leached concentration was several orders of magnitude lower than the extracted and total concentration. This indicates that the mechanisms' surface complexation and/or precipitation are of importance in controlling the elements concentration in neutral waters.

Overall the model predictions for the metal cations Cd, Cu and Zn seem to be adequately determined over a wide range of conditions and without any adjustment of the parameters. This point toward correctly determined active fractions estimated with the Na_2EDTA extractions but also that the mechanisms controlling the solubility of the metals in the ash are not too different compared to in a "normal" soil-solution. The predicted solution concentrations of Pb and Fe were not as well matched with the measurements and emphasises the need for more research on relationship between filter size used in the experiments and colloid particles found in the solution.

At alkaline pH values, precipitation of a mineral phase seemed to be the controlling mechanism for Cu and Zn. However, for the layer with the highest content HFO, the mechanism surface complexation controlled the solution concentrations of Cu and Zn instead. For Cu, precipitation was important also at natural pH values (6.5 – 7.1).

For Zn, the free hydrated ions or ions adsorbed to ferrihydrite dominated the solid-solution partitioning at natural pH.

An aluminium hydroxide was allowed to precipitate and was already at pH 4 controlling the Al concentration in solution.

It was also obvious that competition of reactive surface sites played a great role in determining the amount bound to the sites. Cd, Pb and As had higher affinity for binding to oxide surfaces when minerals of Cu and Zn were allowed to precipitate. The controlling mechanism for Cd, Pb and As seemed to be surface complexation to (hydr)oxides.

At natural pH, ions adsorbed to ferrihydrite dominated the solid-solution partitioning for Pb and As, and for Cd in the layer with the highest ferrihydrite content. For the layers with lower ferrihydrite content, the free hydrated Cd species dominated.

The modelling result for As showed little, or none pH dependency, but since the measurements for As were more often below the detection limit than above, no good verification of the model for the solution concentration could be achieved.

Over all, the model predicted most of the elements concentrations quite well over a wide range of pH values and the model could thus be further used for testing different scenarios and give additional information on how the risk might develop over time. We should however keep in mind that a model is only an approximation of the reality and that conclusions drawn from modelling results will, to some degree, be incorrect.

The results from the kinetics study suggest that a more detailed kinetics study should be made in order to better understand the effect of time on reaction development.

References

ALS Scandinavia, 2015. MG-2 + Sb Metaller i avfall | ALS Scandinavia [WWW Document]. URL http://www.alsglobal.se/miljoe/paket/Avfall_36/Grundaemnen_5/MG-2--Sb-Metaller-i-avfall_17020 (accessed 5.26.15).

Álvarez-Valero, A.M., Sáez, R., Pérez-López, R., Delgado, J., Nieto, J.M., 2009. Evaluation of heavy metal bio-availability from Almagrera pyrite-rich tailings dam (Iberian Pyrite Belt, SW Spain) based on a sequential extraction procedure. J. Geochem. Explor. 102, 87–94. doi:10.1016/j.gexplo.2009.02.005

Ashworth, D.J., Alloway, B.J., 2008. Influence of Dissolved Organic Matter on the Solubility of Heavy Metals in Sewage- Sludge- Amended Soils. Commun. Soil Sci. Plant Anal. 39, 538–550. doi:10.1080/00103620701826787

Bendz, D., 2013. Picture of sampling at Bergvik sulfit.

Bendz, D., n.d. XRD analysis of pyrite ash from Bergvik sulfit.

Berggren Kleja, D., Sverige, Statens Naturvårdsverk, 2006. Metallers mobilitet i mark. Naturvårdsverket, Stockholm.

Degryse, F., Smolders, E., Parker, D.R., 2009. Partitioning of metals (Cd, Co, Cu, Ni, Pb, Zn) in soils: concepts, methodologies, prediction and applications – a review. Eur. J. Soil Sci. 60, 590–612. doi:10.1111/j.1365-2389.2009.01142.x

Dijkstra, J.J., Meeussen, J.C.L., Comans, R.N.J., 2009. Evaluation of a Generic Multisurface Sorption Model for Inorganic Soil Contaminants. Environ. Sci. Technol. 43, 6196–6201. doi:10.1021/es900555g

Dijkstra, J., Meeussen, J.C.L., Comans, R., 2004. Leaching of heavy metals from contaminated soils: An experimental and modeling study. Environ. Sci. Technol. 38, 4390–4395. doi:10.1021/es049885v

Gustafsson, J.P., Pechová, P., Berggren, D., 2003. Modeling Metal Binding to Soils: The Role of Natural Organic Matter. Environ. Sci. Technol. 37, 2767–2774. doi:10.1021/es026249t

Jon Petter Gustafsson, 2014. Visual MINTEQ | Visual MINTEQ – a free equilibrium speciation model.

Lin, Z., Qvarfort, U., 1996. Predicting the mobility of Zn, Fe, Cu, Pb, Cd from roasted sulfide (pyrite) residues—A case study of wastes from the sulfuric acid industry in Sweden. Waste Manag. 16, 671–681. doi:10.1016/S0956-053X(97)00009-3

Mason, R.P., 2013. Trace Metals in Aquatic Systems, 1 edition. ed. Wiley-Blackwell, Hoboken, NJ.

McBride, M.B., 1994. Environmental Chemistry of Soils. Oxford University Press.

Michael E. Essington, 2004. Soil and water chemistry : an integrative approach. CRC Press, Boca Raton, Fla.

Nakhone, L.N., Young, S.D., 1993. The significance of (radio-) labile cadmium pools in soil. Environ. Pollut. 82, 73–77. doi:10.1016/0269-7491(93)90164-J

Naturvårdsverket, 2014. De flesta förorenade områdena är kända [WWW Document]. Naturvårdsverket. URL http://www.naturvardsverket.se/Sa-mar-miljon/Mark/Fororenade-omraden/ (accessed 3.10.15).

Naturvårdsverket, 2012. Preciseringar av Giftfri miljö - miljömål.se [WWW Document]. URL http://www.miljomal.se/sv/Miljomalen/4-giftfri-miljo/Preciseringar-av-giftfri-miljo/ (accessed 2.23.15).

Naturvårdsverket, 1999. Metodik för inventering av förorenade områden.
NFS 2004:10. Naturvårdsverkets föreskrifter om deponering, kriterier och förfaranden för mottagning av avfall vid anläggningar för deponering av avfall.
Nordbäck, J., Tiberg, C., Lindström, Å., 2004a. Karaktärisering av kisaska - Kisaskeförorenade områden i Sverige, Varia 550. Statens geotekniska institut, Linköping.
Nordbäck, J., Wahlström, M., Laerke Jensen, D., 2004b. Användning av extraktionstester för undersökning av metaller i förorenad jord, Varia 545. Statens geotekniska institut.
Ohlsson, Y., Liljemark, A., Carling, M., 2012. Kisaskeutfyllda områden - Strategi och stöd vid riskbedömning. Statens geotekniska institut.
Parfitt, R.L., Childs, C.W., 1988. Estimation of forms of Fe and Al-a review, and analysis of contrasting soils by dissolution and Mossbauer methods. Soil Res. 26, 121–144.
Pédrot, M., Dia, A., Davranche, M., Bouhnik-Le Coz, M., Henin, O., Gruau, G., 2008. Insights into colloid-mediated trace element release at the soil/water interface. J. Colloid Interface Sci. 325, 187–197. doi:10.1016/j.jcis.2008.05.019
Regelink, I.C., Voegelin, A., Weng, L., Koopmans, G.F., Comans, R.N.J., 2014. Characterization of Colloidal Fe from Soils Using Field-Flow Fractionation and Fe K-Edge X-ray Absorption Spectroscopy. Environ. Sci. Technol. 48, 4307–4316. doi:10.1021/es405330x
Riktvärden för förorenad mark [WWW Document], n.d. . Naturvårdsverket. URL http://www.naturvardsverket.se/Om-Naturvardsverket/Publikationer/ISBN/5900/978-91-620-5976-7/ (accessed 5.11.15).
Sposito, G., 2008. The Chemistry of Soils.
Sun, B., Zhao, F.J., Lombi, E., McGrath, S.P., 2001. Leaching of heavy metals from contaminated soils using EDTA. Environ. Pollut. 113, 111–120. doi:10.1016/S0269-7491(00)00176-7
Swedish Standards Institute, 2015. Characterization of waste - Leaching behaviour test - Influence of pH on leaching with continuous pH control.
Swedish Standards Institute, 2012a. Soil quality - Parameters for geochemical modelling of leaching and speciation of constituents in soils and materials - Part 1: Extraction of amorphous iron oxides and hydroxides with ascorbic acid (ISO 12782-1:2012). Swedish Standards Institute.
Swedish Standards Institute, 2012b. Soil quality - Parameters for geochemical modelling of leaching and speciation of constituents in soils and materials - Part 2: Extraction of crystalline iron oxides and hydroxides with dithionite (ISO 12782-2:2012). Swedish Standards Institute.
Swedish Standards Institute, 2012c. Soil quality - Parameters for geochemical modelling of leaching and speciation of constituents in soils and materials - Part 3: Extraction of aluminium oxides and hydroxides with ammonium oxalate/oxalic acid (ISO 12782-3:2012). Swedish Standards Institute.
Swedish Standards Institute, 2015. Characterization of waste - Leaching behavior tests - Influence of pH on leaching with initial acid/base addition.
Swedish Standards Institute, 2003. Characterization of waste - Leaching - Compliance test for leaching of granular waste materials and sludges - Part 2.
Tiberg, C., n.d. EXAFS analysis of pyrite ash from Bergvik sulfit.
Tiberg, C., Sjöstedt, C., Persson, I., Gustafsson, J.P., 2013. Phosphate effects on copper(II) and lead(II) sorption to ferrihydrite. Geochim. Cosmochim. Acta 120, 140–157. doi:10.1016/j.gca.2013.06.012
Zhu, C., Anderson, G.M., 2002. Environmental applications of geochemical modeling. Cambridge University Press, Cambridge ; New York.

Appendix

Comparison simulated and measured concentrations

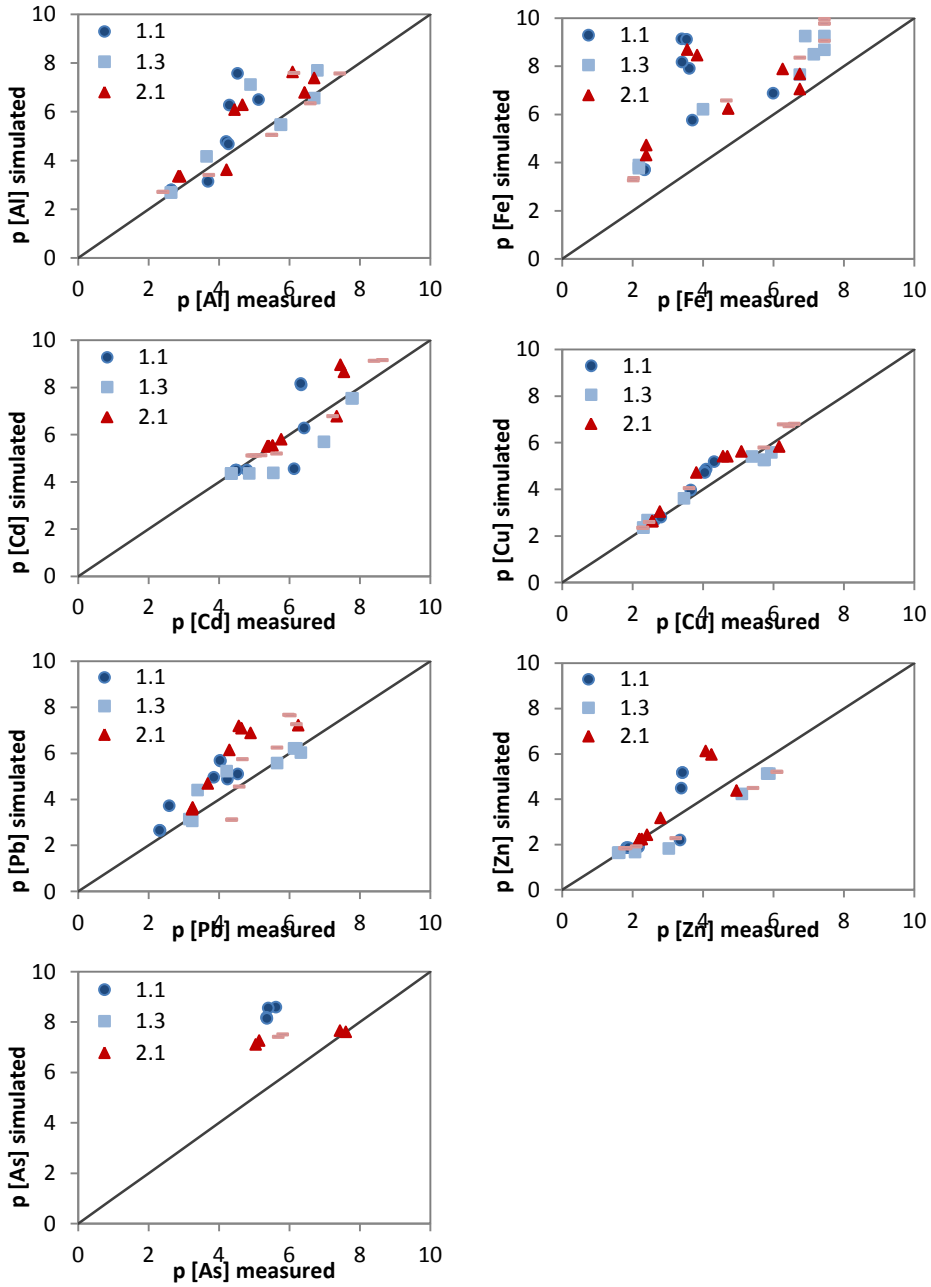

Figure A1. Comparison of simulated total dissolved concentrations of Al, Fe, Cd, Cu, Pb, Zn and As with pH-stat measurements. Concentrations in mol/L. The line represents the perfect 1:1 fit.

Input Visual MINTEQ

Table A1. *Input to Visual MINTEQ for layer 1.1*

1.1	Ca	Fe	Mg	Na	Al	As	Ba	Cd	Cu	Pb	Zn	DOC	SO42-	DIC(CO3)	NO3	K
pH	mg/L	mg/L	mg/L	mg/L	µg/L	µg/L	µg/L	µg/L	µg/L	µg/L	µg/L	mg/L	mg/L	mg/L	mg/L	mg/L
	pH-stat	ox	pH-stat	Added NaOH	ox	ox	pH stat-lowest	EDTA	EDTA	EDTA	EDTA	pH stat - fixed	pH stat - fixed	pH stat - fixed	Added HNO3	pH stat
2.9	89.70	2620	128	100	42600	19700	416	3550	136000	992000	907000	37.3	82.3	0.64	4679	7.01
2.9	89.70	2620	128	100	42600	19700	416	3550	136000	992000	907000	42.9	98.8	1.36	4679	7.01
4.2	89.70	2620	128	0.20	42600	19700	416	3550	136000	992000	907000	8.11	102	1.72	2509	7.01
5.5	89.70	2620	128	0.0001	42600	19700	416	3550	136000	992000	907000	5.8	212	2.11	1800	7.01
7	89.70	2620	128	0.0001	42600	19700	416	3550	136000	992000	907000	18.2	98.3	5.23	1500	7.01
8.5	89.70	2620	128	0.0001	42600	19700	416	3550	136000	992000	907000	51.4	118	11.80	700	7.01
10	89.70	2620	128	0.0001	42600	19700	416	3550	136000	992000	907000	94.7	117	27.30	700	7.01
10.1	89.70	2620	128	0.0001	42600	19700	416	3550	136000	992000	907000	110	116	27.10	700	7.01

Table A2. *Input to Visual MINTEQ for layer 1.3*

1.3	Ca	Fe	Mg	Na	Al	As	Ba	Cd	Cu	Pb	Zn	DOC	SO4	DIC (CO3)	NO3	K
pH	mg/L	mg/L	mg/L	mg/L	µg/L	µg/L	µg/L	µg/L	µg/L	µg/L	µg/L	mg/L	mg/L	mg/L	mg/L	mg/L
	pH-stat	ox	pH-stat	Added NaOH	ox	ox	pH stat-lowest	EDTA	EDTA	EDTA	EDTA	pH stat - fixed	pH stat - fixed	pH stat - fixed	Added HNO3	pH stat
3	91.6	2650	239	0.642	54400	20400	63.2	4945	277000	508000	1515000	19.3	735	1.99	6000	5.73
3	91.6	2650	239	0.642	54400	20400	63.2	4945	277000	508000	1515000	17.9	222	0.98	6236	5.73
4.6	91.6	2650	239	0.642	54400	20400	63.2	4945	277000	508000	1515000	7.72	206	5.48	3619	5.73
5.8	91.6	2650	239	0.000001	54400	20400	63.2	4945	277000	508000	1515000	4.33	409	2.77	3000	5.73
6.9	91.6	2650	239	0.000001	54400	20400	63.2	4945	277000	508000	1515000	3.94	337	3.14	3000	5.73
8.2	91.6	2650	239	0.000001	54400	20400	63.2	4945	277000	508000	1515000	9.42	379	9.3	1000	5.73
9.3	91.6	2650	239	0.000001	54400	20400	63.2	4945	277000	508000	1515000	20	402	13.7	1000	5.73
9.3	91.6	2650	239	0.000001	54400	20400	63.2	4945	277000	508000	1515000	20	370	13.8	1000	5.73

Table A3. *Input to Visual MINTEQ for layer 2.1*

2.1	Ca	Fe	Mg	Na	Al	As	Ba	Cd	Cu	Pb	Zn	DOC	SO4	DIC	NO3	K
pH	mg/L	mg/L	mg/L	mg/L	µg/L	µg/L	µg/L	µg/L	µg/L	µg/L	µg/L	mg/L	mg/L	mg/L	mg/L	mg/L
	pH-stat	ox	pH-stat	Added NaOH	ox	ox	pH stat-lowest	EDTA	EDTA	EDTA	EDTA	pH stat - fixed	pH stat - fixed	pH stat - fixed	Added HNO3	pH stat
3.3	15.7	3620	99.20	150	11700	132800	15.30	343	150000	507000	379000	3.12	62.9	0.25	2494	3.85
3.2	15.7	3620	99.20	300	11700	132800	15.30	343	150000	507000	379000	9.94	428	5.03	2494	3.85
4.3	15.7	3620	99.20	0.32	11700	132800	15.30	343	150000	507000	379000	1.61	54.9	0.25	1130	3.85
5.6	15.7	3620	99.20	0.00001	11700	132800	15.30	343	150000	507000	379000	1.69	141	0.64	1000	3.85
6.5	15.7	3620	99.20	0.00001	11700	132800	15.30	343	150000	507000	379000	1.90	206	0.98	500	3.85
7.3	15.7	3620	99.20	0.00001	11700	132800	15.30	343	150000	507000	379000	3.29	350	2.05	14.1	3.85
8.7	15.7	3620	99.20	0.00001	11700	132800	15.30	343	150000	507000	379000	9.94	428	5.03	14.1	3.85
8.5	15.7	3620	99.20	0.00001	11700	132800	15.30	343	150000	507000	379000	10.20	383	4.95	14.1	3.85

Table A4. *Input to Visual MINTEQ for layer 2.3*

2.3	Ca	Fe	Mg	Na	Al	As	Ba	Cd	Cu	Pb	Zn	DOC	SO4	DIC	NO3	K
pH	mg/L	mg/L	mg/L	mg/L	µg/L	µg/L	µg/L	µg/L	µg/L	µg/L	µg/L	mg/L	mg/L	mg/L	mg/L	mg/L
	pH-stat	ox	pH-stat	Added NaOH	ox	ox	pH stat-lowest	EDTA	EDTA	EDTA	EDTA	pH stat - fixed	pH stat - fixed	pH stat - fixed	Added HNO3	pH stat
2.9	554	2660	323	400	51500	23200	39.3	852	280000	407500	952500	1	2120	0.69	6209	6.15
2.9	554	2660	323	300	51500	23200	39.3	852	280000	407500	952500	1	1610	0.25	6209	6.15
4.5	554	2660	323	0.70	51500	23200	39.3	852	280000	407500	952500	0.66	1580	0.25	2489	6.15
6.1	554	2660	323	0.00001	51500	23200	39.3	852	280000	407500	952500	0.25	1480	1.77	2000	6.15
7.1	554	2660	323	0.00001	51500	23200	39.3	852	280000	407500	952500	0.75	1460	3.23	1000	6.15
8.4	554	2660	323	0.00001	51500	23200	39.3	852	280000	407500	952500	0.56	1380	1	1000	6.15
9.7	554	2660	323	0.00001	51500	23200	39.3	852	280000	407500	952500	0.89	1430	0.94	1000	6.15
9.7	554	2660	323	0.00001	51500	23200	39.3	852	280000	407500	952500	1.11	1660	1.87	1000	6.15